

**Analysis of Potential Applications for the Templated Dewetting of  
Metal Thin Films**

By

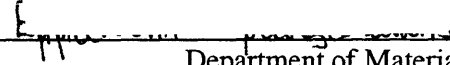
**Emmanouil Frantzeskakis**

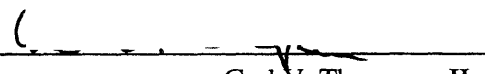
Dipl. Eng. Mining Engineering and Metallurgy  
National Technical University of Athens, 2003


SUBMITTED TO THE  
DEPARTMENT OF MATERIALS SCIENCE AND ENGINEERING  
IN PARTIAL FULFILLMENT OF THE REQUIREMENTS FOR THE DEGREE OF  
MASTER OF ENGINEERING IN MATERIALS SCIENCE AND ENGINEERING  
AT THE  
MASSACHUSETTS INSTITUTE OF TECHNOLOGY  
SEPTEMBER, 2005

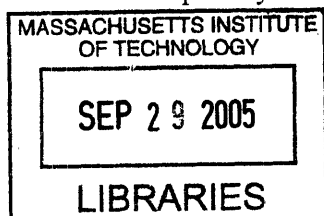
© 2005 Emmanouil Frantzeskakis. All rights reserved.

The author hereby grants to MIT permission to reproduce and distribute publicly paper and  
electronic copies of this thesis document in whole or in part.

Signature of Author:   
Department of Materials Science and Engineering  
August 15, 2005

Certified by:   
Carl V. Thompson II  
Stavros Salapatas Professor of Materials Science and Engineering  
Thesis Advisor

Accepted by:   
Gebrand Ceder  
R.P. Simmons Professor of Materials Science and Engineering  
Chair, Departmental Committee on Graduate Students



ARCHIVES

# **Analysis of Potential Applications for the Templated Dewetting of Metal Thin Films**

By

**Emmanouil Frantzeskakis**

## **Abstract**

Thin films have a high surface-to-volume ratio and are therefore usually morphologically unstable. They tend to reduce their surface energy through transport of mass by diffusion. As a result, they decay into a collection of small isolated islands or particles. This solid-state process, known as thin film dewetting, can be initiated by grooving at grain boundaries or triple junctions.

Dewetting of thin films on topographically modified substrates has many interesting characteristics. It is a novel self-assembly process for the formation of well-ordered nanoparticle arrays with narrow size distributions and uniform crystallographic orientation.

Potential applications of particles resulting from templated thin film solid-state dewetting are reviewed. Applications in patterned magnetic information-storage media, plasmon waveguides, and catalytic growth of ordered arrays of semiconducting nanowires and carbon nanotubes are discussed. Templated dewetting technology has not been fully developed, and technological barriers are identified for all of the commercial applications considered. However, the self-assembly characteristics of templated dewetting may ultimately offer advantages in the manufacture of both patterned media and catalytic nanomaterial growth technologies.

Thesis Advisor: Carl V. Thompson II

Title: Stavros Salapatas Professor of Materials Science and Engineering

## **Acknowledgements**

The successful completion of this thesis would not have been possible without the contribution and help from a lot of different people. First of all, I would like to thank Prof. Carl V. Thompson for his guidance and advice. He made me feel as an important part of his group and he was there to help me when I had problems with the progress of my thesis. I feel proud that I have been a part of the Thompson Group and I wish all the best to its members with their current and future research.

Amanda L. Giermann eagerly shared with me the details of her research. Our regular meetings helped me to proceed with my thesis and provided an answer to my questions. It was very important to know that I had someone with whom I could share every arising problem. I would also like to thank Filip Ilievski and Gilbert Nessim for the helpful discussions.

Congratulations to all the Master of Engineering students of the 2005 class. All the best with your future careers! Special thanks to Kamesh Chilukuri. Kamesh, thank you very much for your help but most importantly thank you for being my friend. I wish you success with your research and I hope to see you soon!

Iwona - thank you for coming with me to the US and staying here for the whole past year. Thank you, for believing in me and cheering me up every time I felt stressed. "Thank you" does not describe all my feelings but I cannot think for any better word right now. We have a whole life together to think about better words!

Finally, I would like to thank my family for believing in me and giving to me all the most important things that I have in life. My parents, Michalis and Nina, and my brother, Paris, have supported me for the past 25 years. I am very lucky that I have you and I am looking forward to seeing you again!

## **Table of Contents**

Abstract.....	2
Acknowledgements.....	3
Table of Contents.....	4
Index of Figures and Tables.....	9
List of Equations.....	11

### **PART I: INTRODUCTION AND DESCRIPTION OF THE TECHNOLOGY..12**

<b>1. Thesis Overview.....</b>	<b>13</b>
<b>2. Background and Description of the Technology.....</b>	<b>15</b>
2.1 Rayleigh Instabilities.....	15
2.2 Dewetting of Metal Thin Films.....	17
2.2.1 The Stability of Defect-Free Films.....	17
2.2.2 The Mechanism of Dewetting.....	18
2.2.3 Experimental Results and Conclusions.....	20
2.3 Templated Dewetting of Metal Thin Films.....	20
2.3.1 Introduction.....	20
2.3.2 Experimental Steps.....	21
2.3.3 Experimental Results.....	23
a) Ordering of Nanoparticles.....	23
b) Size of Nanoparticles.....	26
c) Crystallographic Orientation of Nanoparticles.....	27
2.3.4 Advantages, Limitations and Challenges.....	28
2.3.5 Conclusions.....	32

<b>PART II: ANALYSIS OF POTENTIAL APPLICATIONS.....</b>	<b>35</b>
<b>3. Plasmon Waveguides.....</b>	<b>36</b>
3.1 Introduction.....	36
3.2 Description.....	36
3.3 Optimum Dimensions of the Waveguide.....	37
3.3.1 Optimum Size of the Nanoparticles.....	37
3.3.2 Optimum Spacing of the Nanoparticles.....	38
3.3.3 Other Considerations.....	40
3.4 Dewetting of Nanowires for the Fabrication of Plasmon Waveguides.....	41
3.5 Conclusions.....	42
<b>4. Patterned Magnetic Media.....</b>	<b>45</b>
4.1 Magnetic Media Evolution.....	45
4.1.1 Conventional Magnetic Media – Definition & Limitations.....	45
4.1.2 Patterned Magnetic Media – Definition & Advantages.....	48
4.2 Magnetic Anisotropy.....	51
4.2.1 Magnetic Anisotropy & Magnetic Recording.....	51
4.2.2 Magnetocrystalline Anisotropy.....	52
4.2.3 Shape Anisotropy.....	54
4.2.4 Net Magnetic Anisotropy.....	54
4.3 Limitations of Patterned Media.....	55
4.3.1 Viability Limit.....	55
4.3.2 Superparamagnetic Limit.....	56
4.3.3 Element Interactions – Minimum Interparticle Distance.....	56

4.4	Fabrication of Patterned Media.....	57
4.4.1	Introduction.....	57
4.4.2	Patterning Technologies.....	59
4.4.3	The Use of Lithographic Templates for the Fabrication of Magnetic Elements.....	62
4.4.4	The Uniform Texture of Dewetted Nanoparticles.....	68
4.4.5	The Superparamagnetic Limit of Dewetted Nanoparticles.....	69
4.5	Conclusions.....	71
<b>5.</b>	<b>Catalytic Growth of Semiconducting Nanowires.....</b>	<b>79</b>
5.1	Introduction.....	79
5.2	VLS Growth Mechanism.....	80
5.2.1	Description.....	80
5.2.2	Control of the Growth Direction.....	82
5.3	VSS Growth Mechanism.....	83
5.3.1	Description.....	83
5.3.2	Control of the Growth Direction.....	84
5.4	Conclusions.....	85
<b>6.</b>	<b>Catalytic Growth of Carbon Nanotubes.....</b>	<b>89</b>
6.1	Introduction.....	89
6.2	Synthesis of Carbon Nanotubes.....	91
6.3	Growth Details.....	92
6.3.1	Growth Models.....	92
6.3.2	Growth Conditions – The Role of Dewetting.....	93
6.4	Control of the Growth Direction.....	95
6.5	Conclusions.....	95

<b>PART III: IP ANALYSIS AND BUSINESS MODEL.....</b>	<b>100</b>
<b>7. Intellectual Property.....</b>	<b>101</b>
7.1 Introduction.....	101
7.2 Patents Related to the Fabrication of Topographic Templates.....	102
a) Electron Beam Lithography.....	102
b) X-Ray Lithography.....	102
c) Nanoimprint Lithography.....	103
d) Interference Lithography.....	103
7.3 Patents Related to the Deposition of Thin Films.....	104
a) Electron Beam Evaporation.....	104
b) Sputtering Deposition.....	104
7.4 Patents Related to Rayleigh Instabilities and Thin-Film Dewetting.....	105
7.5 Conclusions.....	107
<b>8. Business Model.....</b>	<b>109</b>
8.1 Empirical Evolution of Technology – Technological Barriers.....	109
8.2 Sustaining and Disruptive Technologies.....	111
8.2.1 Definitions and Examples.....	111
8.2.2 The ‘Death-Zone’ for Start-Up Companies.....	112
8.3 Business Model Proposal.....	114
8.3.1 Commercialization of Patterned Magnetic Media.....	114
a) Patterned Media as a Sustaining Technology.....	114
b) Market Analysis.....	115
c) Patterned Media as a Disruptive Technology.....	117
d) Conclusions.....	118

8.3.2 Commercialization of the Applications Based on Well-Aligned Arrays of Nanowires and Nanotubes.....	119
<b>9. Thesis Conclusions.....</b>	<b>122</b>



## Index of Figures and Tables

<b>Figure 2-1:</b> Decay of an infinite liquid cylinder into a collection of droplets via a Rayleigh instability.....	15
<b>Figure 2-2:</b> SEM images of the fragmentation of a 36 nm-diameter nanowire at three different temperatures.....	17
<b>Figure 2-3:</b> The mechanism of dewetting.....	19
<b>Figure 2-4:</b> A cross-sectional view of the substrate and the deposited thin film during the initial stage of thermal annealing according to the templated dewetting process.....	25
<b>Figure 2-5:</b> The average grain diameter at coalescence vs. the deposition rate.....	30
<b>Figure 2-6:</b> The average grain diameter at coalescence vs. the substrate temperature.....	31
<b>Figure 3-1:</b> The normalized intensity ( $I/I_0$ ) vs. the transmission length of the electromagnetic energy in a plasmon waveguide.....	39
<b>Figure 4-1:</b> Top-view of the basic parts of a conventional hard disk drive.....	45
<b>Figure 4-2:</b> The magnetized grains of a conventional thin film medium.....	47
<b>Figure 4-3:</b> Tracks and bits in a conventional magnetic thin film medium and in a novel patterned medium.....	50
<b>Figure 4-4:</b> Magnetic hysteresis loops when the external magnetic field is applied along an easy and a hard direction.....	52
<b>Figure 4-5:</b> The basic steps of nanoimprint lithography.....	61
<b>Figure 4-6:</b> The principle of interference lithography.....	62
<b>Figure 4-7:</b> Three methods of fabricating patterned media lithographically.....	63
<b>Figure 5-1:</b> Illustration of the VLS growth mechanism.....	81
<b>Figure 5-2:</b> A laser ablation method for the fabrication of Si nanowires.....	81

**Figure 6-1:** A graphene sheet rolled into a single-wall carbon nanotube.....90

**Figure 6-2:** An example of the remarkable mechanical properties of carbon nanotubes.....90

**Figure 6-3:** Four different techniques for the production of carbon nanotubes.....92

**Figure 6-4:** Illustration of a carbon nanofiber.....94

**Figure 8-1:** Empirical evolution of technology.....109

**Figure 8-2:** Chart indicating the ideal and death zones for start-up companies.....113

**Figure 8-3:** History of disruptive technological innovations in the HDD market....118

**Table 2-1:** Experimental steps for the fabrication of the dewetting templates.....22

**Table 2-2:** Experimental steps for the thin-film deposition and annealing.....23

**Table 4-1:** Magnetic anisotropy constants for Fe, Ni and Co, at room temperature...54

**Table 8-1:** Market share of the four largest HDD manufacturers (2004 data).....116

## List of Equations

<b>Equation 2.1:</b> Average center-to-center spacing of the particles fabricated by the agglomeration of one-dimensional structures, according to ‘Rayleigh-Type Instabilities’ and assuming surface diffusion.....	16
<b>Equation 2.2:</b> Average diameter of the particles fabricated by the agglomeration of one-dimensional structures, according to ‘Rayleigh-Type Instabilities’ and assuming surface diffusion.....	16
<b>Equation 2.3:</b> Average grain diameter of a polycrystalline thin film at coalescence..	29
<b>Equation 4.1:</b> Anisotropy energy of materials with uniaxial magnetic anisotropy...	53
<b>Equation 4.2:</b> Anisotropy energy of materials with cubic magnetic anisotropy.....	53
<b>Equation 4.3:</b> Magnetization reversal field.....	56
<b>Equation 4.4:</b> Nearest neighbor interaction field.....	57
<b>Equation 4.5:</b> Magnetization switching rate.....	70

***PART I: INTRODUCTION AND DESCRIPTION OF  
THE TECHNOLOGY***

## 1. Thesis Overview

The main objective of this thesis is to discuss the potential applications of nanoparticles created by the templated dewetting process. Based on experiments by A.L. Giermann and Prof. C.V. Thompson [1, 2], thin film dewetting on surfaces with di-periodic topography seems promising for future commercialization. The discussion focuses on the fabrication of patterned magnetic media, the fabrication of plasmon waveguides and the catalytic growth of semiconducting nanowires and carbon nanotubes. It is the intention of this report to identify the advantages and limitations of the templated dewetting process for the implementation of the above applications.

In the first part of the thesis, the templated dewetting process is described thoroughly. Discussion of the Rayleigh instabilities and the existing research on thin film dewetting provide the necessary background and serve as an introduction to the templated dewetting process.

In the second part of the thesis, potential applications are discussed. The feasibility of the fabrication of plasmon waveguides is directly related to the results determined by the Rayleigh instability theory. The discussion will continue with the description of the advantages and challenges of the templated dewetting process for the fabrication of patterned magnetic media and the catalytic growth of semiconducting nanowires and carbon nanotubes.

In the third part of the thesis, intellectual property is analyzed to identify whether there are any published patents which would hinder the unlicensed commercialization of the templated dewetting process. Finally, a business plan is proposed by identifying the sustaining and disruptive characteristics of the most feasible applications of the templated dewetting process.

## References

1. A.L. Giermann and C.V. Thompson, *Mat. Res. Soc. Symp.*, **818**, p. M3.3.1 (2004).
2. A.L. Giermann and C.V. Thompson, *Appl. Phys. Lett.*, **86**, p. 121903 (2005).

## 2. Background and Description of the Technology

### 2.1 Rayleigh Instabilities

The mechanism of thin film dewetting relies on the formation of capillary instabilities. The problem of capillary instabilities driven by surface energy minimization was first studied by Lord Rayleigh in 1879 [1]. The present section serves as an introduction to the dewetting process by describing the Rayleigh instabilities. Except for the introduction to the dewetting process, the Rayleigh results are directly related to the fabrication of plasmon waveguides by the decay of one-dimensional structures.

Rayleigh used a theoretical analysis to examine the stability of infinite cylinders of not viscous liquids which did not have contact with any surface. He found that the liquid cylinders were unstable to small perturbations with wavelengths  $\lambda$  greater than  $2\pi R$ , where  $R$  is the radius of the liquid cylinder. As a result, they spontaneously decomposed into a collection of liquid droplets (Fig. 2-1). Rayleigh also predicted that perturbations with a wavelength  $\lambda_m=9.016R$  are expected to dominate the above process.

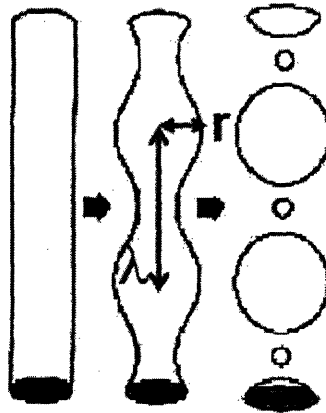


Figure 2-2: Decay of an infinite liquid cylinder into a collection of droplets via a Rayleigh instability [2].

Nichols and Mullins used a similar theoretical analysis to study the stability of solid circular cylinders free of contact with any substrate [3]. They found results identical to Rayleigh. The solid wires were unstable to perturbations with  $\lambda > 2\pi R$  and the wavelength of the dominant perturbations depended on the specific mass-transport mechanism. The only difference is that the decay of the solid wires is a solid-state process and it is not governed by hydrodynamic flow as in the studies of Rayleigh. For surface diffusion, which is expected to dominate in most cases, the following expression holds [3]:

$$\lambda_m = 8.89R. \quad (\text{Eq. 2.1})$$

Assuming that the volume between two consecutive minima forms an island, we can calculate the average diameter of the dewetted nanoparticles as [4]:

$$d = \sqrt[3]{6\lambda_m R} = 3.78R. \quad (\text{Eq. 2.2})$$

The above result was verified by Monte Carlo simulations of a wire decay driven by surface diffusion [4].

According to the above results, one-dimensional structures with radius  $R$  can spontaneously decay due to small variations of their initial radius with  $\lambda > 2\pi R$ . Following equations 2.1 and 2.2, they will form arrays of nanoparticles with average diameter  $d = 3.78R$  and average spacing of  $\lambda_m = 8.89R$ . Annealing promotes atomic diffusion and perturbations can grow in a reasonable amount of time. The higher the annealing temperature, the faster is the decay of the nanowire into a chain of individual particles (Fig. 2-2). Nanowires with large diameters should be annealed at higher temperatures to observe the completion of the process at the same amount of time as for thinner nanowires.



Molares et al. provided experimental evidence of the decay of nanowires with various thicknesses over a range of temperatures [5]. Their results for the spacing and diameter of the fabricated nanoparticles were in fairly good agreement with the theoretical values calculated by Nichols and Mullins [3].

It should be noted that the above analysis does not take into account the effect of the substrate. The wires were modeled as infinite cylindrical lines in free space.

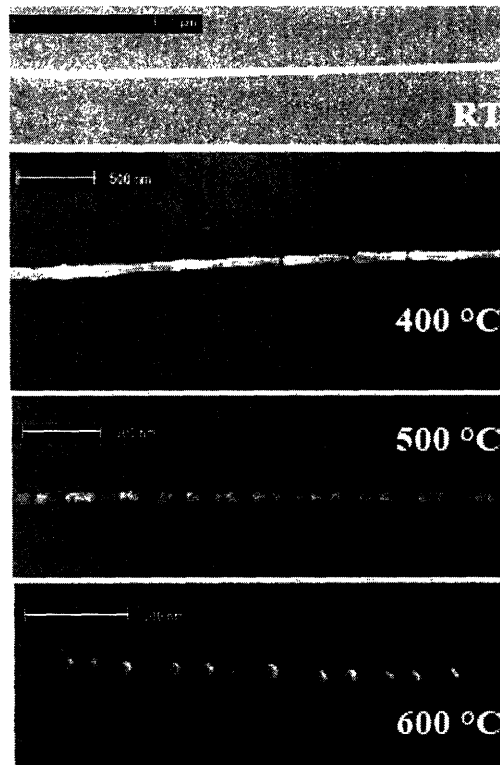


**Figure 2-2: SEM images of the fragmentation of a 36 nm-diameter nanowire at four different temperatures, according to the Rayleigh instability. When the annealing temperature is increased, surface diffusion is enhanced and results in a more rapid decay of the nanowire into a chain of particles [5].**

## 2.2 Dewetting of Metal Thin Films

### 2.2.1 The Stability of Defect-Free Films

As already discussed, an infinite cylinder decomposes into a series of beads after the growth of fluctuations with an amplitude  $\lambda_m$ . However, as shown by Mullins,

a decomposition of a thin film cannot be driven by this kind of instability [6]. A defect-free film is stable to all small perturbations despite its tendency to decrease its surface energy by surface diffusion. Diffusion and decomposition into individual particles can only be possible if perturbations were large enough to penetrate the film and expose areas of the substrate-ambient interface [7].

### **2.2.2 The Mechanism of Dewetting**

Grooving at the grain boundaries and triple junctions of a polycrystalline film is driven by the attempt to minimize the interfacial energy associated with these defects. The grooves can be large enough to reach the substrate. In this case, stable voids can form. Material is transferred from the area of the hole to its periphery by self-diffusion. The void grows by forming a lip with a cylindrical cross-section and a thickened edge (Fig. 2-3a). However, variations of the thickness are observed due to a Rayleigh-type instability of the rim caused by the uneven accumulation of material. According to Jiran and Thompson, as the void grows, it penetrates the thinner areas of the film faster (Fig. 2-3b) resulting in the edge instability mechanism summarized in Figures 2-3c to 2-3f [8]. The result is the decay of the continuous film into individual islands. Taking into account the fact that the void propagates faster through thin areas, the material removed from the substrate is expected to be deposited at stationary areas on either side of the penetrating void tip [8].

The above growth model was proposed by Jiran and Thompson in 1990 for Au thin films [8]. The thin films were deposited by electron beam evaporation and they were subsequent annealed. Annealing enhances atomic diffusion and the dewetting process can be observed in a reasonable amount of time.

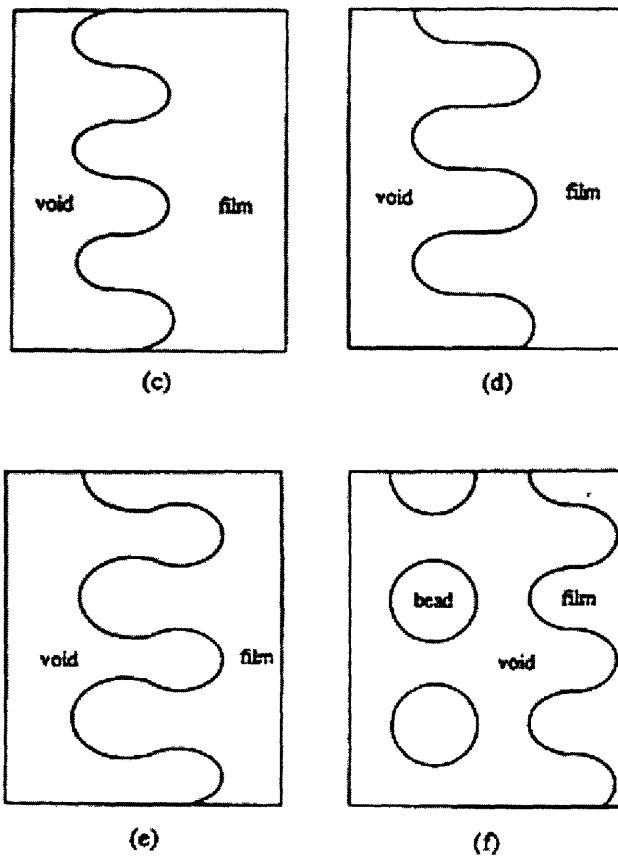
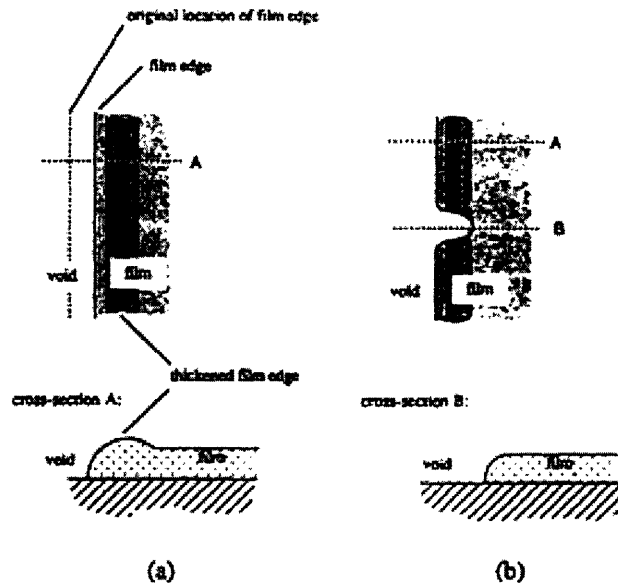


Figure 2-3: a) The film edge is thickened after the transfer of material from the area of hole to its periphery. b) However, perturbations, which correspond to areas with smaller thickness, can grow faster than the rest of the film. c) – f) A series of perturbations which have penetrated the film result from a Rayleigh-type instability of the film edge and finally in the formation of individual beads [8].

### **2.2.3 Experimental Results and Conclusions**

Jiran and Thompson modeled the void growth and predicted a constant growth rate and a thickness dependence of  $h^{-3}$ , where  $h$  is the initial film thickness [8]. The thickness dependence explains the difference propagation velocities of the voids through the thinnest and the thickest areas of the film (Fig. 2-3). In a later study, their work was extended to include the stage of void nucleation in thin film agglomeration [9]. A Johnson – Mehl – Avrami (JMA) analysis was used to calculate the transformation curves for the process. The time required for surface grooves to penetrate the film was considered as the incubation time for the nucleation.

All the above research was conducted by the Materials for Micro- and Nano-Systems (MMNS) Group of the Department of Materials Science and Engineering (DMSE) at MIT during the early 90's. The agglomeration of Au thin films was examined. The above studies in combination with the studies made by different groups verify that dewetting of thin films is a process which can be utilized for the agglomeration of thin films of different materials [10-13].

## **2.3 Templated Dewetting of Metal Thin Films**

### **2.3.1 Introduction**

As it has been already discussed, we can force the self-assembly of nanoparticle arrays by depositing a thin film on a substrate and subsequently annealing it at high temperatures. The film will decompose into a collection of individual islands to decrease its energy. The process is initiated by grooving at grain boundaries or triple junctions and continues via a Rayleigh-type instability.

The self-assembly of nanoparticles by the dewetting process would be of particular interest if we could form ordered arrays of particles. Many potential applications of nanoparticles favor the formation of well-ordered nanoparticle arrays. The objective of this thesis is to discuss the fabrication of patterned magnetic media, plasmon waveguides and the catalytic growth of semiconducting nanowires and carbon nanotubes.

Following the studies by Jiran and Thompson, dewetting of a film on flat substrates results in the formation of nanoparticles with no ordering [8, 9]. This problem was resolved successfully by Giermann and Thompson [14, 15]. According to the novel technology developed by the MMNS Group of the DMSE at MIT, topographically modified substrates were used as templates for the formation of ordered nanoparticle arrays. Surfaces with di-periodic topography controlled the dewetting of thin films and provided a template for the ordering of the fabricated nanoparticles. Moreover, the nanoparticles are topographically confined on the surface. It is speculated that this might prevent coarsening during any high-temperature processing. There are additional advantages of the described technology, in terms of the orientation and the average size of the particles.

### **2.3.2 Experimental Steps**

The first step of the templated dewetting process is the fabrication of the template. {100} Si wafers were used as the substrates and interference lithography was employed as the patterning technique. The fabrication of the templates is explained in detail in table 2-1.

Experimental Steps	Template Fabrication
1.	A masking layer of SiN <sub>x</sub> is grown on a {100} Si wafer
2.	A stack consisting of a XRHi-11 antireflective coating and an OKHA PS4 photoresist is spun onto the substrate
3.	Two laser exposures of a 90° relative orientation are used to create a square array of holes (interference lithography)
4.	Reactive ion etching is used (RIE) to transfer the pattern from the resist to the SiN <sub>x</sub> masking layer
5.	The masked substrate is etched by being immersed in a KOH bath. Wet etching results in the formation of a periodic array of pits (which have the shape of inverted pyramids) bound by the {111} planes
6.	The masking layer is removed
7.	A thin diffusion barrier of SiO <sub>2</sub> is grown on the surface by immersing the substrate in a 3:1:1 HCl:H <sub>2</sub> O:H <sub>2</sub> O <sub>2</sub> solution

**Table 2-1: Experimental steps for the fabrication of the dewetting templates with di-periodic topography [14, 15].**

Templates with three different topographies were fabricated. The first topography had a period of 377 nm and a pit-to-mesa ratio equal to 1.5. The other two topographies had periods of 175 nm and pit-to-mesa ratios equal to 5.3 and 1.9 respectively.

After the fabrication of the substrate, the process continued with the deposition of thin films and their subsequent annealing. Au thin films of three different thicknesses were investigated (16, 21 and 32 nm). Thin films of every thickness were deposited on four different substrates: three topographically modified substrates and a flat Si substrate with a diffusion layer. Therefore, there were twelve different combinations of substrate's topography and initial thickness of deposited film. Table 2-2 summarizes the experimental steps of deposition and annealing.

Experimental Steps	Film Deposition and Dewetting
1.	Au thin films of thicknesses $\approx$ 16, 21 and 32 nm are deposited on all the topographically modified substrates (plus on a flat substrate) by electron beam evaporation
2.	Dewetting is induced by annealing the substrates in air (2h at 850°C)
3.	Scanning electron microscopy (SEM) is used to examine the morphology of the fabricated arrays

**Table 2-2: Experimental steps for thin-film deposition and annealing [14, 15].**

### 2.3.3 Experimental Results

It was demonstrated that the templated dewetting process modifies the characteristics of the fabricated nanoparticles [14, 15]. In the following sections the ordering, size and crystallographic orientation of the particles will be correlated to the experimental parameters (substrate topography and initial thickness of the deposited film).

#### a) Ordering of nanoparticles: Results & Discussion

According to the results obtained by scanning electron microscopy, there were four different nanoparticle morphologies after the dewetting of the Au thin films [14, 15]:

- I. *The particle arrays were random.* This type of behavior was observed for dewetting on flat substrates. However, the same behavior was also observed when the 21 nm and 32 nm films were deposited on the 175 nm-period topography with a wide mesa (pit-to-mesa ratio equal to 1.9). It was clear that

thin films of 21 nm and 32 nm thickness did not interact with the above topography.

II. *There were multiple particles in every pit and larger particles on top of mesas.*

This type of behavior was observed when the 16 nm film interacted with the 377 nm-period and the 175 nm period with narrow mesa (pit-to-mesa ratio equal to 5.3).

III. *There were ordered arrays of one nanoparticle per pit with large particles on mesas.* This was observed when the 21 nm and the 16 nm films were deposited on the 377 nm-period topography and the 175 nm-period topography with a wide mesa respectively.

IV. *There were ordered arrays of one nanoparticle per pit without extraneous and undesired particles.* This was the most desirable type of behavior and the goal of the process. It was observed when the 21 nm thin film was deposited on substrates having a 175 nm-period topography with a narrow mesa. The average diameter of the fabricated nanoparticles was  $120.7 \text{ nm} \pm 1.7 \text{ nm}$ .

The experimental results can be explained by considering the geometry of the thin film during the initial stage of thermal annealing (Fig. 2-4). According to the analysis by Giermann and Thompson, the gold thin film has a positive curvature at point A and a negative curvature at point B [14]. The Gibbs-Thompson equation,  $\Delta\mu = K\gamma V_m$  correlates the excess chemical potential  $\Delta\mu$  to the curvature  $K$  of the surface.  $V_m$  denotes the molar volume and  $\gamma$  the surface energy. Because of the curvature variation, there is a positive excess chemical potential at the edge of the inverted pyramid and a negative  $\Delta\mu$  in the centre of the pyramid. The difference in the chemical potential is the driving force for atom diffusion towards the centre of each



fabricated hole. Atom diffusion will reduce the curvature at the edges and will increase the curvature in the centre of each hole. Eventually, the local curvature at the edges of the pyramid will become so small that it will result in a discontinuous film. As soon as the created grooves intercept the film-substrate interface, dewetting will continue according to the void-edge instability model, which was described by Jiran and Thompson [8].

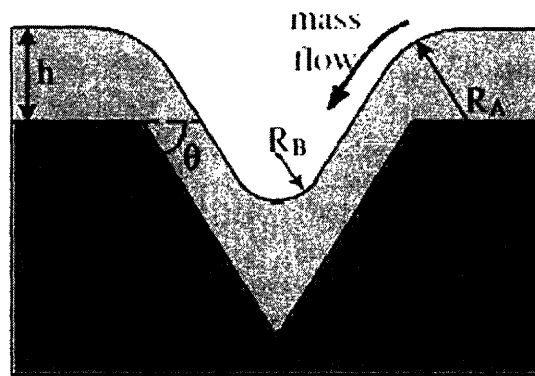


**Figure 2-4:** A cross-sectional view of the film and the substrate at the location of a pit during the initial stage of thermal annealing. Mass flows towards the center of the pit in order to minimize the curvature variations at the surface of the thin film [14].

Type IV morphology can be justified by the above mechanism. In this case, the holes are so close to each other that the high curvature condition exists throughout the mesa width. This condition drives all the material off the mesas and into the holes, resulting in the most desired type of behavior.

This is not possible if the mesas are too wide. In such a case, the thin film is flat in the centre of the mesas and therefore there is no driving force for diffusing the whole amount of material into the centre of the pits. This material will remain on the mesas resulting in Type III morphology.

Type II morphology is observed when the gold film is very thin. Such a thin film may be discontinuous even before the annealing process, due to imperfections during the deposition technique. There can already be some grooves on the sidewalls or in the centre of each pyramid. When the film is annealed these random grooves result in the formation of nanoparticles in a random manner. Therefore, we observe multiple particles per pit with no ordering.

When the initial film is too thick relative to the size of the pyramids, the thin film dewets as if it was deposited on a flat substrate ignoring the surface topography (Type I morphology). Very large film thickness results in very small curvature at the edge of the holes, which in turn yields a very small driving force for diffusion. Therefore, there are no atoms diffusing towards the centre of the pits and the thin film dewets as if deposited on a flat surface.

#### **b) Size of Nanoparticles: Results & Discussion**

Another advantage of the described technology is that it results in the reduction of the average particle size in comparison to nanoparticles created on flat substrates. Results were confirmed by SEM and can be summarized as following [15]:

- I. The average particle size decreased by about 75% in the case of the desired dewetting behavior, which yielded a single nanoparticle per hole.
- II. The average particle size decreased by about 60% even when the fabricated particles did not interact with the substrate's topography.

The above phenomenon can be explained by the kinetics of Rayleigh instabilities. As already discussed, the dewetting process relies on Rayleigh-type

instabilities formed around the edge of the film. The topography of the substrate modifies the curvature of the receding film. The instabilities on a templated surface have a shorter length scale than the instabilities on a flat surface. Therefore, templated dewetting results in the creation of particles with smaller average diameters.

### **c) Crystallographic Orientation of Nanoparticles: Results & Discussion**

The crystallographic orientation of nanoparticles was investigated using the pole figures obtained by the XRD technique [15]. When a polycrystalline Au thin film is deposited on a flat substrate, it develops a strong {111} texture as a result of the interfacial energy minimizing condition [16]. However, it will exhibit random in-plane orientation.

For particles created by dewetting of a film on a flat substrate, the above two observations are still valid. However, the results were very different for particles created by dewetting on a substrate with di-periodic topography. XRD pole figures provided clear evidence that the fabricated particles developed a {100} crystallographic texture with uniform in plane orientation [15].

The fabricated particles have their <111> crystallographic directions normal to the sides of the pyramidal pits, due to the interfacial energy minimizing condition. The crystallographic texture of the thin films is determined by the normal to the plane of the substrate. Taking into account the angle of the pits ( $54.7^\circ$ ), it was easily determined that the direction normal to the substrate is of the <100> type [15]. This means that the fabricated particles have developed {100} texture (instead of {111} on a flat surface).

In-plane orientation is speculated to be a further result of the fact that the fabricated particles have their <111> directions normal to the sides of the pits because

of the surface energy minimizing condition [15, 16]. In contrast to the deposition of a polycrystalline film on a flat substrate, in-plane orientation is well-determined by the geometry of the pits.

#### **2.3.4 Advantages, Limitations and Challenges**

According to the above experimental results, the templated dewetting process has many advantages. First of all, it results in the perfect ordering of the fabricated nanoparticle arrays. Secondly, the particles have uniform in-plane and out-of-plane orientation. Moreover, their average diameters are smaller than the corresponding values on a flat substrate. Finally, the topographical confinement of the nanoparticles might prevent coarsening or agglomeration during subsequent high temperature processing.

A disadvantage of the described technology is that its resolution is so far limited by the resolution of the patterning technique. Another limitation of the dewetting process is that perfect ordering can be only achieved by decay of a continuous thin film (patch or strip). Otherwise, the ordering of the fabricated particles will not follow the topographical features of the template. However, very thin films are expected to be discontinuous. Since the size of the dewetted particles is expected to be determined by the thickness of the deposited film, the above consideration poses a minimum limit on the size of the well-ordered fabricated nanoparticles.

Deposition of continuous thin films with very small thicknesses is a future challenge and plays a crucial role in the templated dewetting process. According to C.V. Thompson, film thickness at which coalescence occurs is about half of the average grain size at coalescence, assuming that the formed grain boundaries are

immobile [17]. Therefore, thin films with small average grain diameter,  $\bar{d}$ , are desirable for the templated dewetting process, since they coalesce at a smaller thickness,  $h$ .

Polycrystalline thin films form through three successive steps. First, stable clusters are nucleated on a substrate. Secondly, these clusters grow by the adsorption of adatoms and finally they coalesce yielding a polycrystalline continuous film. C.V. Thompson modeled the above process and found that the average grain diameter at the point of coalescence can be approximated by the following equation [17]:

$$\bar{d} = 1.351\delta + 1.203 \left( \frac{G_o}{I} \right)^{\frac{1}{3}}. \quad (\text{Eq. 2.3})$$

$\delta$  denotes the width of a circular zone around a nucleated island in which any atom will diffuse to that island instead of desorbing or forming a new cluster.  $I$  is the nucleation rate and  $G_o$  is a temperature-independent term, which is involved in the growth rate equation.

$G_o$  is directly proportional to the rate of deposition  $F_{\text{dep}}$ , while  $I$  is proportional to  $F_{\text{dep}}^{n^*}$  [17]. The critical cluster size  $n^*$  is in the order of 2 in physical vapor deposition techniques [18]. Therefore,  $G_o/I$  decreases with increasing deposition rate. The width of the circular zone  $\delta$  is independent of  $F_{\text{dep}}$ . At low rates of deposition, the second term of equation 2.3 dominates and thus the average grain diameter decreases with increasing  $F_{\text{dep}}$ . At high rates of deposition, the first term of equation 2.3 dominates and  $\bar{d}$  is independent of  $F_{\text{dep}}$  [17]. The results are summarized in Figure 2-5. High deposition rates are desirable in order to obtain a continuous thin film at a smaller thickness.

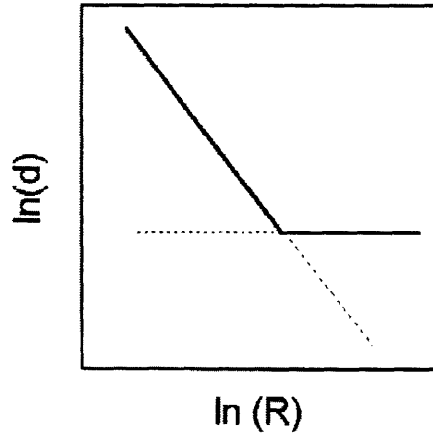


Figure 3-5: The average grain diameter,  $d$ , at coalescence vs. the deposition rate,  $R$  [17].

Except for the deposition rate, the average grain diameter depends on the substrate temperature,  $T$ . Higher temperatures enhance adatom diffusion to the nucleated clusters, resulting in grains with larger diameters at the point of coalescence. When the substrate temperature is lower, adatoms have lower mobilities and they tend to form new islands rather than diffuse to the previously nucleated clusters [18]. Therefore, the average grain diameter at the point of coalescence is smaller. Figure 2-6 illustrates the dependence of  $\bar{d}$  on the temperature of the substrate. The natural logarithm of  $\bar{d}$  is proportional to  $1/T$  within regimes. The changes of the proportionality constant are due to the increase of  $n^*$  with increasing temperature [17]. In conclusion, the minimum thickness of a continuous thin film is expected to decrease if we cool the substrate during the deposition process.

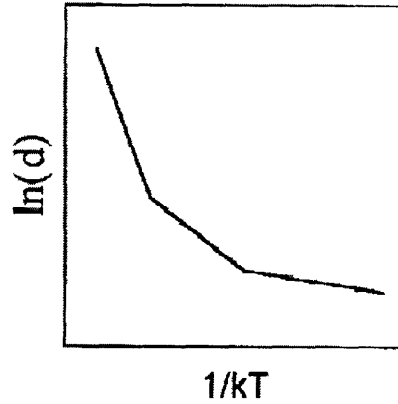


Figure 2-6: The average grain diameter,  $d$ , at coalescence vs. the substrate temperature,  $T$  [17].

Moreover, the background pressure during evaporative or sputter deposition affects the average grain diameter and the film thickness at coalescence. At high pressures the deposited atoms lose energy through collisions with impurity atoms. Therefore, they have low mobilities resulting in a continuous film at a smaller thickness [18]. The same effect has an increase in the sputtering gas pressure [18].

The minimum thin film thickness depends on the melting temperature of the deposited material [18]. The melting point of a material reflects its binding energy. Strongly bound solids have a high melting temperature. In this case, it is more difficult for the deposited atoms to bind to an existing cluster. Therefore, thin films of materials with high melting temperatures tend to be continuous at a smaller thickness.

In conclusion, there are many modifications of the deposition process which can yield a continuous thin film with smaller thickness. Following these modifications, we can scale-down the templated dewetting process. A high deposition rate is desirable. In evaporative deposition,  $F_{\text{dep}}$  can be increased by increasing the source temperature, while in sputter deposition by applying a higher target-substrate bias. The substrate temperature should be maintained as low as possible during each deposition process. Moreover, a high background pressure is desirable, since it results

in adatoms with low mobilities. In the case of sputtering, sputtering gas with a high pressure contributes to the above result. Finally, thin films of materials with high melting temperatures are expected to result in a further decrease of the minimum film thickness.

### **2.3.5 Conclusions**

The combination of dewetting with interference lithography provides us with a novel route for fabricating well-ordered nanoparticle arrays. The simplicity and low cost of the interference lithography coupled with the self-assembly characteristics of dewetting is very promising for large scale fabrication.

The objective of this thesis is to focus on the dewetting stage of the process and discuss the implementation of a few potential applications. Although emphasis will be given on the combination of dewetting with interference lithography, other patterning methods will be considered as well. Templated dewetting can be regarded as a novel method for transferring a pattern to the desired material. It can be therefore considered as a substitute for evaporation and lift-off, electrodeposition on patterned electrodes, or etching.

The unique advantages of the templated dewetting process are very promising for a range of applications. The current limitations encountered at this early stage of explorations are expected to be overcome with continuous scientific research and future modifications of the process.



## References

1. L. Rayleigh, *Proc. London Math. Soc.*, **10**, p. 4 (1879).
2. C. Trautmann, "Micro- and nanostructuring with energetic heavy-ions",  
website: [www.nsc.ernet.in/events/NSC\\_WORKSHOP](http://www.nsc.ernet.in/events/NSC_WORKSHOP)
3. F.A. Nichols and W.W. Mullins, *Trans. Metall. Soc. AIME*, **233**, p. 1840 (1965).
4. T. Müller, K.H. Heinig and B. Schmidt, *Mat. Sci. Eng. C*, **19**, p. 209 (2002).
5. M.E. Toimil Molares, A.G. Balogh, T.W. Cornelius, R. Neumann and C. Trautmann, *Appl. Phys. Lett.*, **85**, p. 5337 (2004).
6. W.W. Mullins, *J. Appl. Phys.*, **30**, p. 77 (1959).
7. D.J. Srolovitz and S.A. Safran, *J. Appl. Phys.*, **60**, p. 247 (1986).
8. E. Jiran and C.V. Thompson, *J. Electron. Mater.*, **19**, p. 1153 (1990).
9. E. Jiran and C.V. Thompson, *Thin Solid Films*, **208**, p. 23 (1992).
10. D.J. Srolovitz and S.A. Safran, *J. Appl. Phys.*, **60**, p. 255 (1986).
11. D.C. Agrawal and R. Raj, *Acta Metall.*, **37**, p. 2035 (1989).
12. F.Y. Genin, W.W. Mullins and P. Wynblatt, *Acta Metall. Mater.*, **40**, p. 3239 (1992).
13. R. Dannenberg, E.A. Stach, J.R. Groza and B.J. Dresser, *Thin Solid Films*, **370**, p. 54 (2000).
14. A.L. Giermann and C.V. Thompson, *Mat. Res. Soc. Symp.*, **818**, p. M3.3.1 (2004).
15. A.L. Giermann and C.V. Thompson, *Appl. Phys. Lett.*, **86**, p. 121903 (2005).
16. C.V. Thompson, *Annu. Rev. Mater. Sci.*, **30**, p. 159 (2000).
17. C.V. Thompson, *J. Mater. Res.*, **14**, p. 3164 (1999).

18. C.V. Thompson, Massachusetts Institute of Technology, 3.48J Lecture Notes  
(2004).

***PART II: ANALYSIS OF POTENTIAL  
APPLICATIONS***

### **3. Plasmon Waveguides**

#### **3.1 Introduction**

Conventional optical elements, such as dielectric waveguides, suffer from two serious limitations, which hinder their miniaturization. First of all, their size is limited by the diffraction limit of light [1]. This limit is about half the wavelength of the transmitted light. Therefore, for visible light this translates into a minimum element size of a few hundred nm. Another serious limitation is that complex guiding geometries, such as  $90^\circ$  corners, are not possible [2]. Plasmon waveguides are structures which can overcome the above limitations and guide electromagnetic energy in a coherent fashion via arrays of closely spaced metal nanoparticles. Their function relies on exploiting non-propagating fields of electromagnetic radiation [1].

Well-ordered nanoparticle arrays created by the technology of dewetting are potential candidates for the guidance of electromagnetic energy. The goal of this section is to discuss the challenges associated with the use of one-dimensional arrays of dewetted nanoparticles for fabricating plasmon waveguides.

#### **3.2 Description**

Metal nanoparticles interact with light at their resonance frequency due to the excitation of a collective motion of their conduction electrons. Energy is drawn into the particle because of its strong polarization [2]. The collective motion of the electrons is known as a surface plasmon polaritons (SPP). The intensity of SPPs is maximized at the surface of the nanoparticles and decays exponentially away from it. The evanescent fields of SPPs can exceed the optical excitation intensity by several orders of magnitude [1]. The particles should be much smaller than the wavelength of

light in order to achieve in-phase excitation of all the electrons. Nanoparticles in the order of 30 – 50 nm have been effectively used to guide electromagnetic energy [2]. Noble metals (Ag, Au, Cu) are of a particular interest, since their resonance frequencies lie in the visible range of light [2-4].

Electromagnetic energy is transferred along the nanoparticle chain in the form of plasmon oscillations taking advantage of the near-field electrodynamic interactions [1]. The first particle of the chain is irradiated by an external light field and gives rise to an SPP field with very high intensity near the illuminated particle. All the other particles get their plasma oscillation by coupling. The second particle is situated within the intense near-field created by the first particle and it picks up the optical excitation. Electromagnetic energy is transferred by the same way, all along the chain.

### **3.3 Optimum Dimensions of the Waveguide**

#### **3.3.1 Optimum size of the Nanoparticles**

Because interest in plasmon waveguides is relatively recent, there has so far been no agreement on the optimum size of the used nanoparticles. However, the particles should fulfill two necessary conditions in order to allow efficient transfer of electromagnetic energy. They must be small enough, much smaller than the wavelength of the incident light, to achieve in-phase excitation of all the electrons, while at the same time they must be large enough to avoid enhanced damping due to surface scattering of the conduction electrons [2, 3].

It has been demonstrated that gold and silver nanoparticles with diameters between 30 and 50 nm satisfy the above conditions. Therefore, gold and silver

particles in the above size regime have been used as building blocks for the fabrication of plasmon waveguides [2-4].

### 3.3.2 Optimum Spacing of the Nanoparticles

The importance of regular particle spacing can be justified after a short overview of the damping mechanisms, which are encountered during the energy transfer along plasmon waveguides. Intensity loss can be due to three different reasons: inelastic surface scattering of the conduction electrons, radiation losses into the far-field and internal damping due to resistive heating. As already mentioned, the surface scattering effect can be minimized by working with nanoparticles having dimensions above a minimum limit. Moreover, radiation losses into the far-field are negligible because of the dominance of the near-field coupling mechanism. Therefore, the main reason for intensity loss is internal damping of the surface plasmon polaritons due to resistive heating. The dominance of the near-field coupling mechanism and its strong dependence on distance underline the importance of regular particle spacing [2, 3].

Quinten et al. have modeled the intensity decay vs. the transmission length for variations in the spacing of the particles [4]. Their analysis focused on Ag nanoparticles with 50 nm diameters. Maier et al. used the results obtained from the above modeling to propose two different methods for the fabrication of plasmon waveguides based on Au nanoparticles with diameters between 30 and 50 nm [2]. According to the simulation, the minimum transmission loss is observed for a center-to-center distance of  $3r$ , where  $r$  is the radius of the nanoparticles. Quinten et al. predicted a signal attenuation coefficient of  $\gamma=1.1\times 10^6 \text{ m}^{-1}$ , which corresponds to 2.4 dB/500 nm. Brongersma et al. calculated analytically a value of 3 dB/500 nm, which

is in close agreement [3]. Intensity follows an exponential decay. Transmission loss is higher for particles which are more closely spaced. It reaches which is 2.3 times than at zero interparticle distance. The transmission loss is also higher for arrays with interparticle distances greater than  $3r$ . In this case, the intensity decay is non-exponential.

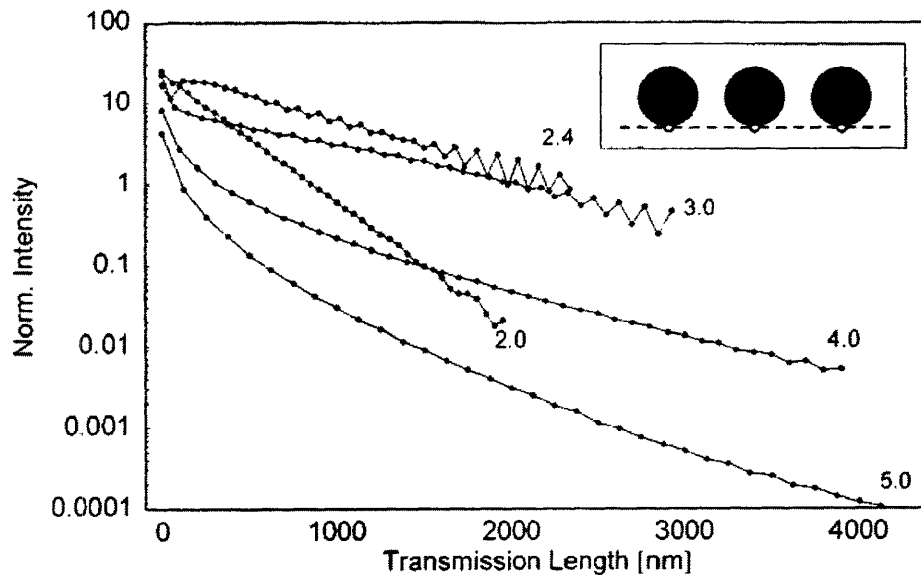


Figure 3-1: The normalized intensity ( $I/I_0$ ) vs. the transmission length of the electromagnetic energy in a plasmon waveguide based on a regular array of Ag nanoparticles with 50 nm diameters. The numbers on each plotted line correspond to the different values of center-to-center spacing of the particles [4].

Figure 3-1 summarizes the results obtained from the numerical simulation of Quinten et al. [4]. The various plotted lines correspond to different center-to-center spacing (see inset of Figure 3-1) of the nanoparticles. The starting values of normalized intensity can be higher than 1 because of the resonantly enhanced field of the first nanoparticle. We can see that even for the optimum spacing, efficient propagation is limited to a few  $\mu\text{m}$  at best. Therefore, rather than acting as waveguides in the conventional sense, which supports practically lossless light

propagation, nanoparticle arrays could be used as local devices focusing optical fields down to nanoscale volumes.

### 3.3.3 Other Considerations

The shape of the nanoparticles has an effect on the velocity of the energy propagation (group velocity). For example, since ellipsoids can be spaced closer together than spheres of the same volume, the group velocity along an array of ellipsoids is higher than for an array of spheres of equivalent volume [3]. Moreover, it is important that the fabrication method can produce nanoparticles of a narrow size and shape distribution, since position and width of the dipole resonance depend on these two factors [3]. Variations of the location and width of the dipole resonance can lead to inefficient transfer because of the strong distance dependence of the near-field coupling mechanism.

The choice of host matrix can also be important for various reasons. The term 'host matrix' refers to the ambient of nanoparticles deposited on a surface. A poor choice of a matrix can result in significant damping because the plasmons can couple to various degrees of freedom in the host. Moreover, by varying the refractive index ( $\eta$ ) of the matrix, we can shift the resonance wavelength over several hundred nm. Finally, an increase in  $\eta$  can decrease the coupling strength between the particles and thus reduce the group velocity [3]. The refractive indices of air and vacuum ( $\eta=1.00029$  and  $\eta=1.0$  correspondingly) are expected to work well for the fabrication of plasmon waveguides [2, 3].



### 3.4 Dewetting of Nanowires for the Fabrication of Plasmon Waveguides

The process of dewetting must be combined with a patterning technology (e.g. lithography) in order to produce nanoparticle arrays necessary for the fabrication of plasmon waveguides. We need a patterning technology capable of fabricating one-dimensional structures with feature sizes determined by the capillary instability [5-8].

The simplest plasmon waveguide could be fabricated by the dewetting of a single line. However, in order to fabricate a device based on waveguides, we need to have a complicated waveguide pattern. Interference lithography cannot be a candidate for patterning, since it is not capable of patterning complex waveguide patterns required for the fabrication of a completed circuit. Dewetting should therefore be combined with electron beam lithography, X-Ray lithography or any other kind of patterning technology capable of producing one-dimensional, non-periodic structures, which can dewet to form nanoparticles with sizes in the range of 30 to 50 nm.

For the analysis of this section we will consider the simplest case, which is the dewetting of a nanowire deposited on a substrate. This is a different type of templated dewetting technology than that described in section 2.3. There is no substrate with topographical features. The dewetting process is instead confined in a one-dimensional track patterned using a lithographic technique. We will base our analysis on the results determined by Nichols for the instability of infinite cylinders of solid materials, which are free from any surface contact [8]. These results were summarized in section 2.1 of this thesis. It should be noted again that we are ignoring the effect of the substrate on determining the fastest growing wavelength of perturbations.

A serious disadvantage of the dewetting technology for the fabrication of plasmon waveguides arises from the consideration of the average spacing determined by the capillary instability [5-8]. Following the analysis presented in section 2.1, and

considering the above-stated assumption, we can calculate the diameter and spacing of the nanoparticles fabricated by the dewetting of a nanowire. The average diameter of the fabricated particles and the average center-to-center spacing are related to the initial wire radius  $R$  by the previously stated equations 2.1 and 2.2.

According to equation 2.2, we could obtain dewetted particles in the 30-50 nm regime if we could pattern one-dimensional structures with initial radii between 8 and 13 nm. After a straightforward calculation (substituting  $R$  with  $d/3.78$  in equation 2.1), we find that the average center-to-center spacing of the fabricated nanoparticles is equal to  $4.7r$ , where  $r$  is their diameter. According to figure 3-1, plasmon waveguides with such a large spacing will suffer from huge intensity losses even if the transmission length is as small as a few hundred nanometers. Such an array would be only suitable for short-range optical addressing of individual nanoparticles. Dewetting can produce nanoparticles with regular spacing and narrow size and shape distributions; however the disadvantage of the large interparticle distances predominates over the advantage of the achievable uniformity.

### **3.5 Conclusions**

The dewetting process of one-dimensional structures for the fabrication of plasmon waveguides suffers from one major disadvantage. The dewetted nanoparticles are more widely spaced ( $4.7r$ ) than the optimum distance ( $3r$ ). Therefore, intensity loss is increased and the process is considered as a bad candidate for waveguide fabrication.

Many different techniques have been proposed for the construction of nanoparticle waveguides. Maier et al. have demonstrated two different techniques [2]. The first method is a combination of electron beam lithography and lift-off, while the

second relies on the manipulation of randomly deposited nanoparticles using an AFM tip. A novel self-assembly technique for the fabrication of plasmon waveguides was proposed by McMillan et al. and relies on the use of nanoscale templates made of chaperonin proteins [9].

It should be noted that the technology of plasmon waveguides is still at an embryonic stage and many questions remain unanswered. All investigations of the optical properties of the waveguides have so far been confined to collective excitations [10-12]. No direct measurement of electromagnetic energy transport along the nanoparticle chains has yet been made.

## References

1. J.R. Krenn, *Nature Mater.*, **2**, p. 210 (2003).
2. S.A. Maier, M.L. Brongersma, P.G. Kik, S. Meltzer, Ari A.G. Requicha and H.A. Atwater, *Adv. Mater.*, **13**, p. 1501 (2001).
3. M.L. Brongersma, J.W. Hartman and H.A. Atwater, *Phys. Rev. B*, **62**, p. R16356 (2000).
4. M. Quinten, A. Leitner, J.R. Krenn and F.R. Aussenegg, *Opt. Lett.*, **23**, p. 1331 (1998).
5. T. Müller, K.-H. Heinig and B. Schmidt, *Mat. Sci. Eng. C*, **19**, p. 209 (2002).
6. M.E. Toimil Molares, A.G. Balogh, T.W. Cornelius, R. Neumann and C. Trautmann, *Appl. Phys. Lett.*, **85**, p. 5337 (2004).
7. L. Rayleigh, *Proc. London Math. Soc.*, **10**, p. 4 (1879).
8. F.A. Nichols and W.W. Mullins, *Trans. Metall. Soc. AIME*, **233**, p. 1840 (1965).
9. R.A. McMillan, C.D. Paavola, J. Howard, S. L. Chan, N. J. Zaluzec and J. D. Trent, *Nature Mater.*, **1**, p. 247 (2002).
10. J.R. Krenn, A. Dereux, J.C. Weeber, E. Bourillot, J.P. Goudonnet, G. Schider, W. Gotschy, A. Leitner, F.R. Aussenegg and C. Girard, *Phys. Rev. Lett.*, **82**, p. 2590 (1999).
11. S.A. Maier, M.L. Brongersma, P.G. Kik and H.A. Atwater, *Phys. Rev. B*, **65**, p. 193408 (2002).
12. S.A. Maier, P.G. Kik and H.A. Atwater, *Appl. Phys. Lett.*, **81**, p. 1714 (2002).

## 4. Patterned Magnetic Media

### 4.1 Magnetic Media Evolution

#### 4.1.1 Conventional Magnetic Media – Definition & Limitations

Magnetic data storage is widely used in applications like audio tapes, video cassette recorders, computer hard disks, floppy disks and credit cards. Hard disks and floppy disks are also referred as rigid magnetic media to distinguish them from the magnetic tapes. Nowadays, magnetic hard disk recording is the most widely used of all the magnetic storage technologies. Hard disk recording remains the primary and most economical means of data storage in today's computer. Advances in the speed of a microprocessor are always accompanied by advances in storage capacity, contributing to the enhancement of the capabilities of modern computers.

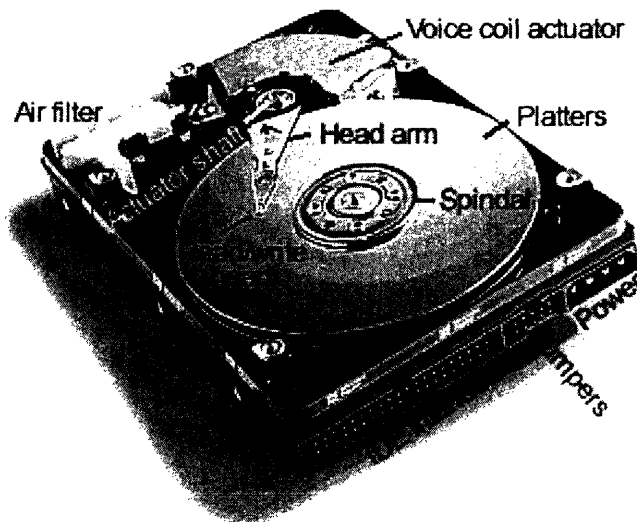
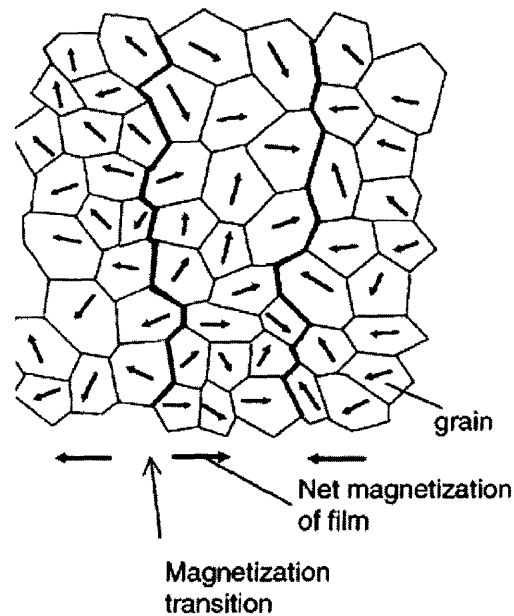


Figure 4-1: Top-view of the basic parts of a conventional Hard Disk Drive (HDD). A HDD can contain one or more magnetic hard disks (platters) [1].

A conventional magnetic medium (e.g. a hard disk) consists of four layers; a substrate, an underlayer, a magnetic film where the data is stored, and a protective overcoat. The magnetic thin film is usually a polycrystalline alloy of cobalt, chromium and platinum (or tantalum), which is sputtered at elevated temperatures [2, 3]. The above alloy is used due to its high magnetic anisotropy. During magnetic recording, an external magnetic field is applied by the writing head. Data is stored in concentric circles, which are called 'tracks'. Small areas of the track (bits) are magnetized parallel or antiparallel to the track direction (Fig. 4-3). Since the magnetization of the recording bits lies in the plane of the film, the prevailing technology of thin film media is also known as longitudinal recording. During the reading process, the reading head detects magnetic fields coming from places where the magnetization changes. If a magnetic field is present, stored data is interpreted as '1'; if a magnetic field is absent, it is interpreted as '0' [2, 4]. In order to increase the amount of information the drive can store, most HDDs have multiple hard disks (platters) and magnetic heads (Fig. 4-1).

Each bit of the polycrystalline thin film consists of many grains, which are created during the deposition process. The grains behave as tiny magnets whose magnetization can be flipped by the writing head during the data writing process. In conventional magnetic media, the overall signal-to-noise ratio (SNR), is expected to be determined by the transition noise originating from irregularities in the magnetization transitions at the bit boundaries (Fig. 4-2). These irregularities become very sharp if the bits of the polycrystalline thin film contain few grains. Therefore, the number of grains,  $N$ , within a single bit determines the signal-to-noise ratio of the medium. It has been demonstrated that SNR is proportional to  $N^{1/2}$  [3, 8]. Thus, as the number of bits and consequently the density of the medium increase, an acceptable

SNR can be only achieved by maintaining a large number of grains within each bit. To keep the noise small enough for reliable data detection, roughly 50~100 grains are needed per bit [3]. To achieve a reduction of the bit size, we should therefore decrease the average grain size.



**Figure 4-2: The magnetized grains of a conventional thin film medium. Magnetic noise arises because of the magnetization transitions between two adjacent bits [2].**

However, when the grains become very small their magnetization is subject to thermal fluctuations. This phenomenon is well known as the superparamagnetic limit and can be quantified by the ratio  $KV/kT$  [2, 5].  $K$  denotes the net magnetic anisotropy of the grain,  $k$  the Boltzmann constant,  $V$  the grain volume and  $T$  is the temperature of operation. This stability criterion is valid for magnetic media with uniaxial magnetic anisotropy. For a thermally stable medium, the accepted values of the above ratio are on the order of 60 [2, 3, 50, 51]. For longitudinal thin film media, the superparamagnetic effect is expected to occur at densities of 6 – 15 Gbit/cm<sup>2</sup> [2].

To overcome the limit determined by the stability ratio, we should either decrease the temperature of operation, or increase the anisotropy of the medium. Temperature could be theoretically decreased down to cryogenic values but operation at such small temperatures would be a complicated process for current magnetic media and electronic devices. Moreover, an increase in  $K$  would result in an increase in the coercivity of the medium, which would in turn require stronger writing fields. Therefore, a paradigm shift is required to overcome the limitations of longitudinal thin film media.

#### **4.1.2 Patterned Magnetic Media – Definition & Advantages**

Two different approaches, which could overcome the thermal limitations, have been demonstrated. Perpendicular recording aligns the magnetization of the bits vertically, perpendicular to the disk, which allows additional room on a disk to pack more data; thus, enabling higher storage capacities. The demagnetizing fields the bits exert upon each other are smaller than in longitudinal recording. Therefore, perpendicular media enjoy five times greater thermal stability limits than longitudinal media, where the bits are aligned horizontally, parallel to the surface of the disk. It has been estimated that perpendicular media can reach up to  $150 \text{ Gb/cm}^2$  capacities [2].

The fabrication and use of patterned magnetic media is an even more revolutionary approach. The term patterned media refers to media for which each bit consists of an isolated piece or grain of magnetic material. They are arranged periodically to be synchronized with a signal channel, which is an external magnetic field. The periodic arrangement can be achieved using high-resolution lithography or a templated self-assembly technique. It should be noted that a magnetic element (bit) is a single magnetic domain. It could be formed either by one grain or by several



grains, whose magnetization is dependent on the magnetization of surrounding grains. These grains are called 'exchange coupled' grains. On the other hand, thin film media consists of a collection of grains, which behave as tiny magnets with independent magnetization (random decoupled grains) [3].

Patterned media have two important advantages over conventional thin film media. First of all, they eliminate the noise associated with multigrain bits and magnetization transitions (Fig. 4-2, Fig. 4-3), since the magnetic bits are defined by the physical patterning and not by the grain boundaries between two oppositely magnetized regions. Moreover, the thermal stability ratio,  $KV/kT$ , refers to the volume and the anisotropy of the entire element and not to individual grains. Since we do not longer need on the order of 100 grains per bit, but just one single grain-sized switching volume, the bit size can be significantly smaller. Density can be increased by roughly two orders magnitude compared to conventional recording media. Patterned media are expected to give storage densities exceeding  $150 \text{ Gb/cm}^2$  [2, 7].

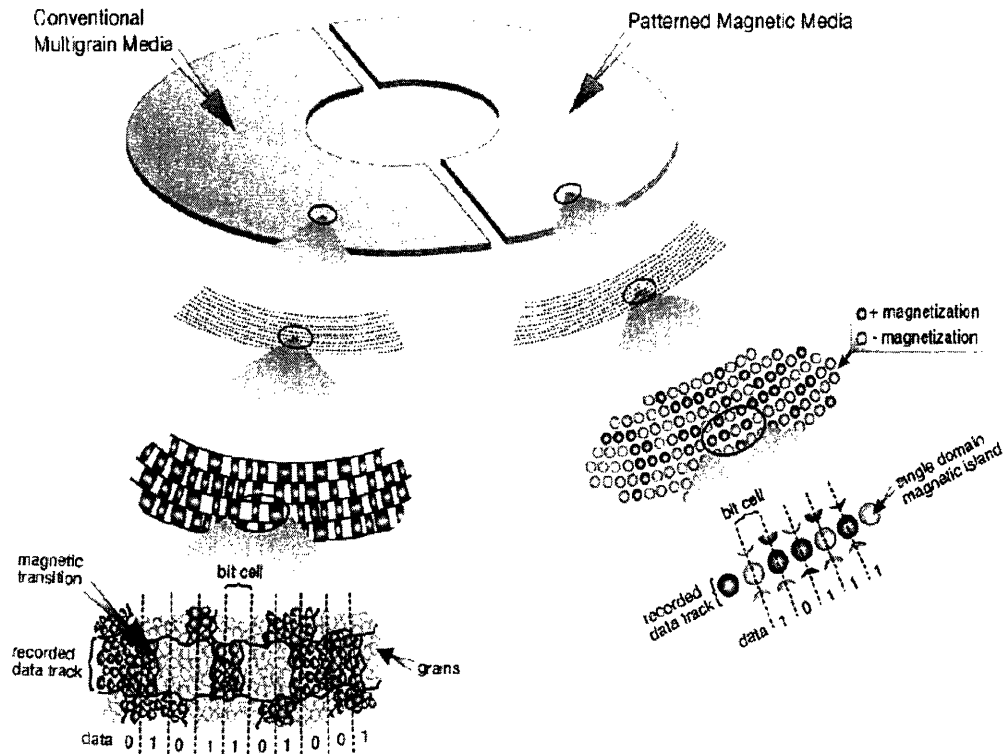


Figure 4-3: Tracks and bits in a conventional magnetic thin film medium and in a novel patterned medium. The magnetization transitions between the bits of a patterned medium are avoided because the bits are defined by the patterning process [3].

Nanoparticles fabricated by the templated dewetting process of a magnetic thin film are potential candidates for the fabrication of patterned magnetic media. We will discuss the feasibility of this application by identifying the relevant limitations and challenges of templated dewetting. The desired dimensions and crystallographic orientation of the magnetic nanoparticles are determined by the limitations of patterned media and the magnetic anisotropy theory. Therefore, before we discuss the advantages and disadvantages of the dewetting technology for the fabrication of magnetic media, we should first identify the importance of magnetic anisotropy and the inherent limitations of the patterned media.

## 4.2 Magnetic Anisotropy

### 4.2.1 Magnetic Anisotropy & Magnetic Recording

The term magnetic anisotropy,  $K$ , refers to the dependence of the magnetic properties on the crystallographic direction in which they are measured. It expresses the tendency of magnetization to lie along certain crystallographic directions, or easy axes, in a magnetic material. The magnetic properties of every material can be quantified by the magnetization curves, or hysteresis loops. The magnetization curves depend strongly on the magnetization direction.

For magnetic data storage we need two stable states of opposite magnetization,  $M$ . Moreover, the magnetic field,  $H$ , required to switch between them should be well defined. The above conditions can be only achieved if the hysteresis loop of the magnetic material is almost square (Fig. 4-4a). As already discussed, magnetization tends to align itself along easy axes. If an external magnetic field is applied along a hard axis, it quickly rotates the magnetization along the field direction. However, as soon as the field is removed, the magnetization rotates back into the easy direction. As a result, there is no hysteresis (Fig. 4-4b). If the magnetization axis coincides with the easy axis of the material, hysteresis is observed (Fig. 4-4a) and square magnetization loops can be achieved [4]. Therefore, for storage media, the particles must all be aligned with their easy axes parallel to the direction of the writing field. Any deviation from perfect alignment results in a loss of squareness. A perfect square loop is never achieved due to the interactions between particles and the distribution of their switching fields (see figure 4-4c) [2]. The squareness of the hysteresis loop is a measure for the suitability of the magnetic media. It is defined by the ratio of the

magnetization when the external field has been removed (remnant magnetization or  $M_r$ ) to the maximum value of magnetization (saturation magnetization or  $M_s$ ).

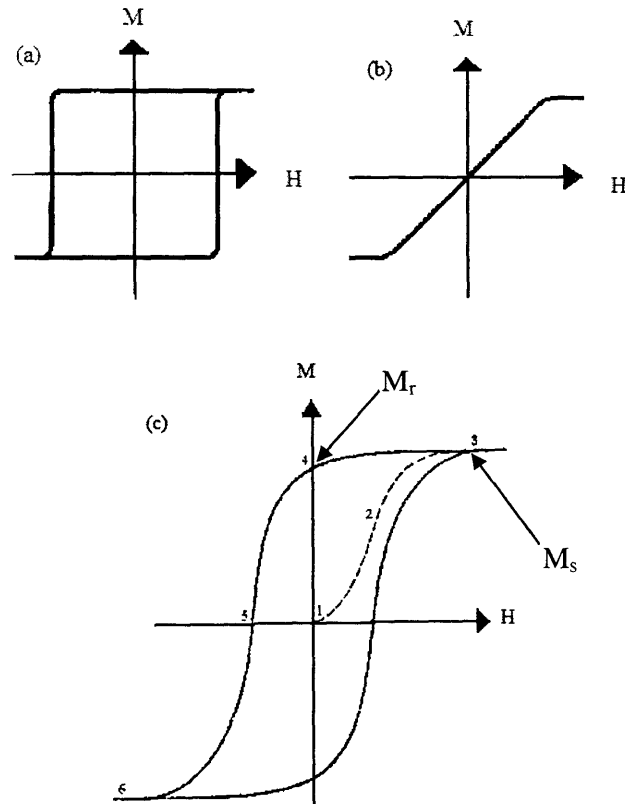


**Figure 4-4: Magnetic hysteresis loops. (a)** when the magnetization axis coincides with the easy axis (perfect square loop). **(b)** when the magnetization axis coincides with a hard axis. **(c)** typical sheared magnetization loop taking into account the interactions between particles and the distribution of their switching fields [4].

#### 4.2.2 Magnetocrystalline Anisotropy

There are two contributors to the magnetic anisotropy: magnetocrystalline anisotropy,  $K_m$ , and shape anisotropy,  $K_s$ , [2]. Magnetocrystalline anisotropy is the tendency of magnetization to align along a preferred crystallographic orientation. The preferred crystallographic orientation, which coincides with the easy axes if we neglect shape effects, are the  $\langle 100 \rangle$  directions for body-centered cubic magnetic materials (e.g. Fe), the  $\langle 111 \rangle$  directions for face-centered cubic magnetic materials (e.g. Ni) and the axis of six-fold symmetry (c-axis or  $[0001]$  direction) for hexagonal

close-packed magnetic materials (e.g. Co) [4]. A polycrystal with no preferred orientation of its grains does not have magnetocrystalline anisotropy.

The phenomenon that a material has only one ‘easy axis’ in its lattice, is known as ‘uniaxial magnetic anisotropy’. For materials with uniaxial anisotropy, such as Co, the anisotropy energy can be approximated as [4]:

$$E = K_1 \sin^2 \theta + K_2 \sin^4 \theta \quad (\text{Eq. 4.1})$$

A cubic material without shape anisotropy has more than one ‘easy axes’ in its lattice. This phenomenon is a result of the cubic symmetry and is known as ‘cubic magnetic anisotropy’. For materials with cubic anisotropy, the anisotropy energy E can be written as a series of expansion of the direction cosines,  $\alpha_i$ , of the saturation magnetization relative to the crystal axes. The following approximation is usually used [4]:

$$E = K_1 (\alpha_1^2 \alpha_2^2 + \alpha_2^2 \alpha_3^2 + \alpha_3^2 \alpha_1^2) + K_2 (\alpha_1^2 \alpha_2^2 \alpha_3^2) \quad (\text{Eq. 4.2})$$

$K_1$  and  $K_2$  are called anisotropy constants and their values are summarized in Table 4-1. It should be noted that Co exhibits much higher values of magnetocrystalline anisotropy than Fe or Ni. For cubic materials the following sign convention is used to define the easy axis of magnetization;  $K_1 > 0$  implies easy  $\langle 100 \rangle$  directions, while  $K_1 < 0$  implies easy  $\langle 111 \rangle$  directions [5]. In section 4.4.5, the values of the anisotropy constants will be used to calculate the minimum size of Co, Ni, and Fe particles which yield a thermally stable magnetic medium.

Material	$K_1$ (J/m <sup>3</sup> )	$K_2$ (J/m <sup>3</sup> )
Fe (cubic anisotropy)	$4.8 \times 10^4$	$-1.0 \times 10^4$
Ni (cubic anisotropy)	$-4.5 \times 10^3$	$-2.3 \times 10^3$
Co (uniaxial anisotropy)	$4.1 \times 10^5$	$1.5 \times 10^5$

**Table 4-1: Magnetic anisotropy constants for Fe, Ni and Co at room temperature.**

### 4.2.3 Shape Anisotropy

If the magnetic particles are not spherical, then it will be easier to magnetize along the long axis of the particle [4]. This phenomenon is known as shape anisotropy and it occurs due to the demagnetizing field of the particles. Shape anisotropy has a large effect in the determination of the net magnetic anisotropy. It should be added to the magnetocrystalline anisotropy, taking into account the orientation of the anisotropy axes [2].

Patterned media relying on shape anisotropy include: electrodeposited Ni pillars, CVD grown Fe pillars, evaporated Co ellipses, etched ellipses of a Co/Cu multilayer etc. [2]. In the case of pillars, we have an easy out-of-plane magnetization axis, while in the case of ellipses, the easy magnetization axis lies in-plane

### 4.2.4 Net Magnetic Anisotropy

It is desirable, that the easy axis determined by magnetocrystalline anisotropy coincides with the long axis of the particle. In this case, the two anisotropy factors simply add up in determining the net magnetic anisotropy of the element. If however, the long axis of a non-spherical particle does not coincide with the preferred direction

determined by magnetocrystalline anisotropy, then the easy axis of its net magnetic anisotropy will be determined by the dominating anisotropy factor.

In the case of nickel nanoparticles, the magnetocrystalline anisotropy is usually negligible and net anisotropy is determined by their shape [34]. The effect of aspect ratio on the magnetic anisotropy of Ni patterned media was examined in detail by Farhoud et al. [6]. They used interference lithography and lift-off to fabricate nickel nanoparticles with a variety of diameters and aspect ratios. The change from in-plane to out-of-plane net anisotropy was observed when the aspect ratio had values higher than 0.65. This means that the small out-of-plane magnetocrystalline anisotropy affects the net anisotropy of the particles, but the shape anisotropy dominates for most of the aspect ratios [6].

Cobalt has much higher magnetocrystalline anisotropy than nickel (Table 4-1). New et al. have fabricated polycrystalline cobalt islands with shape anisotropy using electron beam lithography and ion milling [35]. They concluded that, for small particles the shape anisotropy is not large enough to determine the easy axis of magnetization. The critical size was approximated at 150nm [35]. New et al, suggest that a solution to this problem could be to increase the aspect ratio of the particles. However, particles with higher aspect ratios would be difficult to magnetize [35].

### **4.3 Limitations of Patterned Media**

#### **4.3.1 Viability Limit**

A patterned medium will be competitive only if it offers much higher storage capacities than the conventional longitudinal thin film media. Hard drives based on the prevailing longitudinal media technology can reach densities up to 15 Gbit/cm<sup>2</sup>.

Therefore, patterned media must reach densities of more than 30 Gbit/cm<sup>2</sup> to be competitive. It has been proposed [2], that arrays with a 50 nm period are required in order to achieve densities of 40 Gbit/cm<sup>2</sup> [7].

#### **4.3.2 Superparamagnetic Limit**

As has already been mentioned, the stability criterion for patterned media applies to the anisotropy and volume of a single magnetic element. Although superparamagnetic behavior is expected for much higher densities than for conventional thin film media, magnetic nanoparticles of very small sizes still suffer from superparamagnetism. This is because they have such small volumes that they fail to yield an acceptable value to the stability ratio. The minimum size of a thermally stable patterned medium, according to the criterion of superparamagnetism, can be calculated by considering the anisotropic constants of the medium. The relevant analysis will be made for Co, Ni and Fe nanoparticles in section 4.4.5.

#### **4.3.3 Element Interactions – Minimum Interparticle Distance**

For magnetic fields applied parallel to the easy axis, the field required to reverse the particles' magnetization is given by [2,7]:

$$H_{sw}=2K/\mu_0M_s. \quad (\text{Eq. 4.3})$$

$H_{sw}$  is known as the switching field of the particle,  $K$  is the net magnetic anisotropy,  $M_s$  is the saturation magnetization, and  $\mu_0$  is the permeability of vacuum. Considering out-of-plane magnetization, the nearest neighbor interaction field is [2, 7]:



$$H_i = M_s V / 4\pi\mu_0 d^3. \quad (\text{Eq. 4.4})$$

$V$  is the volume of the particles and  $d$  their center-to-center spacing. Assuming a square array of particles, the total magnetic field acting on any particle is equal to  $9H_i$  [2, 7].

The magnetization of one element can be reversed without affecting its neighbors if its switching field exceeds the maximum interaction field from all neighbors. It has been demonstrated that a stable patterned medium is achieved when the magnetic elements have diameters on the order of half of the period of the array, or smaller [7]. According to the viability limit, which was discussed in section 4.3.1, if we want to achieve sufficiently high recording density, feature sizes of 25 nm are required.

Interactions between particles, as well as the distribution of their switching fields, shear the hysteresis loop. Owing to these effects, a perfect square hysteresis loop is almost never observed. Switching field distributions are a result of the intrinsic variability between particles, due to small differences in shape, size, and microstructure. It can be minimized by improving the uniformity of the array, which requires good control over the lithographic or self-assembly fabrication process.

## **4.4 Fabrication of Patterned Magnetic Media**

### **4.4.1 Introduction**

The preceding analysis of the characteristics and limitations of patterned magnetic media will serve as a basis for identifying the advantages, disadvantages, and challenges of the templated dewetting process in fabricating a viable and stable

patterned medium. The role of dewetting can be more easily analyzed after a short overview of the whole range of technologies for the fabrication of magnetic media.

In order to commercially manufacture a patterned medium, any fabrication technique should be able to produce an array of magnetic elements with periodicity less than 50 nm at low cost. For the fabrication of magnetic elements with a periodic structure a patterning method (e.g. lithography) must be combined with a technique which can transfer the desired pattern to the magnetic material. Depending on their mechanism, the pattern transferring processes can achieve resolutions of a lithographic or of a sub-lithographic length scale.

The following sections will serve as an overview of the lithographic methods and the pattern transferring processes, which have been proposed for the fabrication of patterned magnetic media. Electron beam lithography, X-Ray lithography, nanoimprint lithography and interference lithography have been used for the fabrication of magnetic media [2, 14, 15, 23-29]. Lithographic patterning is usually followed by a conventional pattern transferring process such as etching, electrodeposition or evaporation and lift-off [7, 9-19]. However, nanoscale patterns of magnetic materials can be created using a combination of conventional lithography and a self-assembly process. These self-assembly processes can decrease the minimum achievable feature size. Examples include the phase separation of block copolymers, the formation of ordered pores in anodized alumina films and the dewetting of metal thin films.

#### 4.4.2 Patterning Technologies

##### a) Electron Beam Lithography

Electron beam lithography uses a finely focused beam of electrons which can be deflected accurately and precisely over a surface [36]. When the surface is coated with a radiation sensitive polymer, the electron beam can be used to write patterns of very high resolution. The high resolution of electron beam lithography is due to the fact that it is not limited by diffraction, as in the case of conventional optical lithography. There are three main types of electron beams employed for e-beam lithography: the Gaussian spot, the variable shaped beam and cell projection. Cell projection has the advantage that it can pattern complex geometric shapes in one exposure with an e-beam system [37].

Electron beam lithography is the most widely used patterning method for fabricating magnetic nanostructures with dimensions of 15 nm and higher [14, 15, 23-28]. Its main advantage is the capability of making patterns of arbitrary geometry. Using the combination of electron beam lithography and lift-off, magnetic elements of a lot of different shapes, such as rectangles, ellipses, rings, and wires, have been demonstrated [14, 15, 24, 25]. Moreover, electrodeposition has been used to form columns of magnetic materials [23, 26-28] and etching to fabricate magnetic dots with in-plane and out-of-plane anisotropy [38].

The main disadvantage of electron beam lithography is that it is a serial method with a very low throughput. Although it has been extensively used for patterning small areas, it is unsuitable for large-area samples and its high cost prevents its commercialization.

## **b) X-Ray Lithography**

Soft X-rays with wavelengths in the range of 1 to 10 nm represent another alternative source with potential for high resolution pattern replication into resist materials. The subsequent development of the resist leaves a nanoscale template.

X-Ray lithography has been used to pattern large-area samples. Feature sizes as small as 20 nm can be possible [2]. For commercial application a synchrotron source is used to enable high throughput. It should be noted that the mask for X-Ray lithography is fabricated by electron beam lithography. However, the large number of replications made of each mask justifies the additional experimental step.

## **c) Nanoimprint Lithography**

In nanoimprint lithography, a thermoplastic polymer is spun onto a substrate where the nanostructures are to be fabricated. Secondly, a rigid mold is pressed onto the polymer layer and causes its deformation. In the third step, the mold is separated from the patterned polymer leaving the desired nanoscale templates [24].

Magnetic features as small as 10 nm dots with 40 nm period have been demonstrated using evaporation followed by lift-off [24], while 70 nm Ni pillars have been fabricated by electrodeposition [29, 39]. The rigid mold is produced by electron beam lithography and it can be used for a large number of replications. The cost of nanoimprint lithography is lower than e-beam lithography and X-Ray lithography. Commercial imprinting machines are under development by Molecular Imprints Inc. [30].

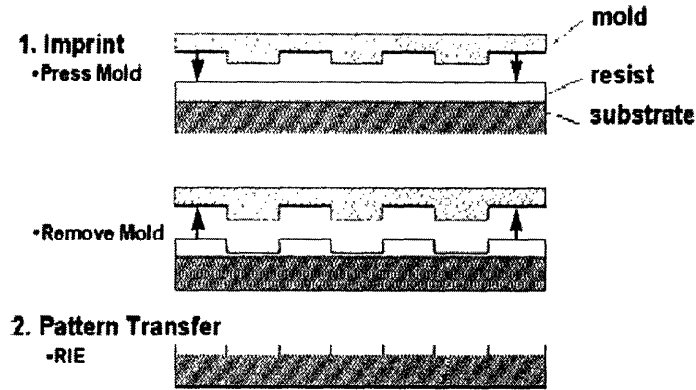


Figure 4-5: The basic steps of nanoimprint lithography [24].

#### d) Interference Lithography

Interference lithography (IL) is a low-cost method ideal for patterning large-area structures. It is a maskless lithographic process based on the interactions of laser beams. A laser beam is split and recombined on a resist to form a pattern of fringes. A second exposure at a  $90^\circ$  relative orientation to the first is carried out to produce a perpendicular set of fringes. The resulting grid pattern defines an array of holes or dots.

The resolution of interference lithography is in the order of 180-200 nm. The patterning method has been combined with lift-off to fabricate magnetic arrays of Ni and Co [7, 16, 40, 41]. Moreover, electrodeposition has been demonstrated for the fabrication of magnetic pillars [7], while etching for the fabrication of magnetic dots and ellipses [7, 42]. To produce smaller features, the use of achromatic interference lithography (AIL) is required [2]. AIL has been used to produce 100 nm period patterns [31] and it is expected to be extended to 50 nm period features.

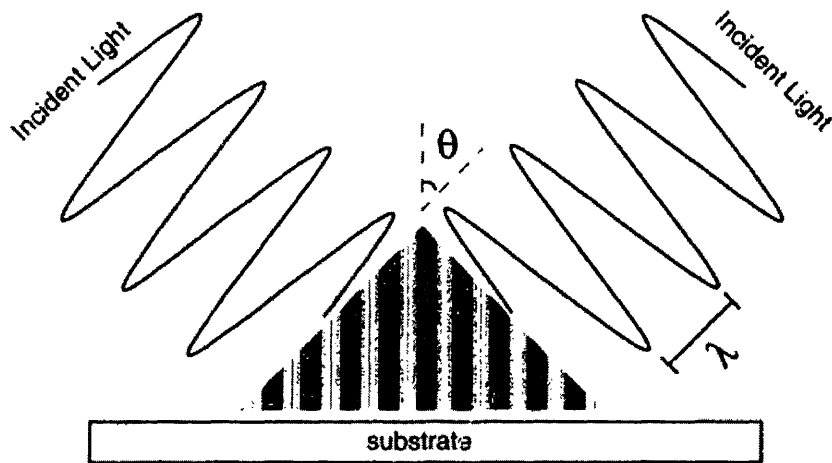


Figure 4-6: The principle of interference lithography. Two laser beams, with wavelength  $\lambda$  and at a relative orientation  $\theta$ , interfere to form a pattern of fringes on a substrate. The period of the pattern is equal to  $\lambda/(2\sin\theta)$  [22].

#### 4.4.3 The Use of Lithographic Templates for the Fabrication of Magnetic Elements

##### a) Etching of Magnetic Thin Films

Etching is considered a subtractive process because magnetic material is deposited prior to lithographic patterning and it is then etched to form the desired nanoscale pattern. As already discussed, it can be combined with any of the above lithographic processes in order to fabricate discrete magnetic elements of arbitrary shapes. Etching provides the widest choice of materials and microstructures. The minimum feature size of the fabricated elements is determined by the resolution of the patterning technique. Ion milling is used instead of reactive ion etching, because most magnetic materials are difficult to etch using RIE [17-19].

## **b) Evaporation and Lift-Off**

Evaporation followed by lift-off is considered an additive process, since magnetic material is deposited after patterning. It is one of the most widely used methods for the generation of magnetic nanoparticle arrays. Evaporation can follow any of the above-mentioned patterning techniques to fabricate flat (e.g. ellipses), tapered (e.g. pyramids) or conical particles from ferromagnetic metals and alloys [13-16, 24, 25].

## **c) Electrodeposition**

In electrodeposition the substrate serves as a cathode in an electrolytic cell. It is an additive process, which has been widely used to fabricate magnetic nanoparticles with high aspect ratios (e.g. pillars). As a result, electrodeposited nanoparticles can have very high values of shape anisotropy. Electrodeposition has been proposed for pure metals such as Ni and Co, alloys and multilayers [7, 9-12, 24].

The mechanisms of etching, lift-off and electrodeposition are summarized in Figure 4-7. The three conventional techniques for transferring nanoscale patterns to the desired magnetic material are capable of fabricating elements with sizes determined by the lithographic process. The combination of lithographic patterning with novel self-assembly techniques, has been proposed to fabricate magnetic elements of a sub-lithographic length-scale with long-range order.

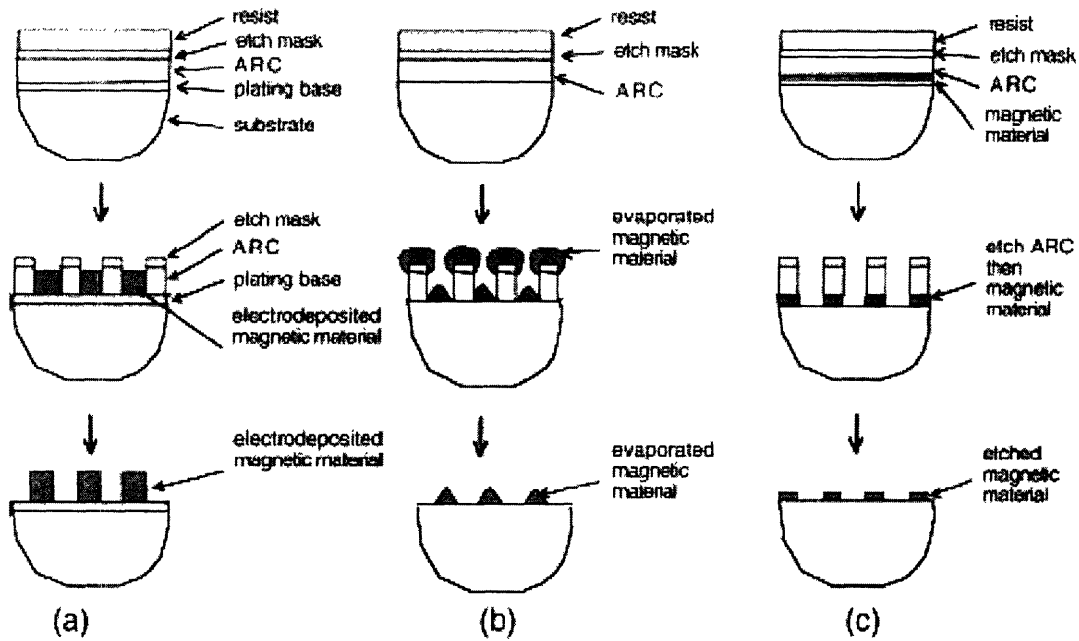


Figure 4-5: Three methods of fabricating patterned media lithographically. (a) Electrodeposition of magnetic material on a template. (b) Evaporation of magnetic material on the same template followed by lift-off. (c) Etching of a pre-deposited magnetic material [2].

#### d) Templated Self-Assembly Using Block Copolymer Lithography

Block copolymers (BCP) consist of two segments of chemically distinct polymer chains, which are connected by a covalent bond. These incompatible polymer blocks cannot phase separate on a macroscopic level, since they are covalently interconnected. As a result, BCP form periodic arrays of lamellar, cylindrical or spherical nanodomains, typically in the range of 10-100 nm. The size and geometry of the domains depend on the relative molecular weights of the two polymers [37]. Small feature size and spacing of BCP nanodomains helps them to serve as novel lithographic masks.

The fabricated periodic patterns have good short-range order. However, their long-range order is poor, limiting their potential for the fabrication of patterned magnetic media. Topographically modified substrates have been used to induce



orientation and long-range ordering of the polymer domains [43-45]. This process, which was first introduced by Segalman et al. [46] is referred as templated self-assembly or graphoepitaxy of block copolymer films.

With respect to the fabrication of patterned media, research has been focused on the formation of magnetic dot arrays by taking advantage of the microphase separation of sphere-forming block copolymers. For example, circumferential gratings of magnetic dots have been fabricated by a combination of nanoimprint lithography, block copolymer separation and ion milling [44]. Moreover, templated self-assembly of cylinder-forming block copolymers has attracted significant scientific interest. Xiao et al. have recently proposed the fabrication of well-ordered cobalt dot arrays by the self-assembly of an asymmetric diblock copolymer on topographic templates fabricated by electron beam lithography. The block copolymer was phase separated into cylindrical nanodomains, which served as masks for the subsequent deposition of cobalt [43].

The combination of block copolymer separation with conventional lithography is promising for the fabrication of patterned media with a sub-lithographic length-scale. The size of the polymer domains is about an order of magnitude smaller than the width of the initial lithographic pattern. A disadvantage of the templated block copolymer lithography is that the spacing of the arrays and the size of the fabricated elements are not uniform near the edges of the topographical features.

#### **e) Templated Self-Assembly Using Ordered Porous Alumina**

When aluminum is anodized, the resulting alumina film forms an arrangement of long and columnar nanopores with typical diameters from 4 to 300 nm [47]. Excellent hexagonal ordering of the fabricated pores has been observed within

restricted domains. Although the size of these domains can be increased with longer anodization [33], the pores lack long-range order.

The combination of a conventional lithographic technique with the self-organization process of porous alumina films has been proposed for the fabrication of square or hexagonal arrays of pores which exhibit long-range order [53, 54]. Their remarkable stability makes them useful as novel lithographic masks for the deposition of a variety of nanostructures, such as nanodots, nanowires, and carbon nanotubes.

With respect to the fabrication of magnetic media, porous alumina templates have been used for the electrodeposition of cobalt nanowires [10, 32, 33]. Moreover, Krishnan et al. have recently proposed the combination of interference lithography and self-organization of porous alumina to evaporate nickel catalysts for the subsequent growth of carbon nanotubes [47].

The combination of the self-organization process of porous alumina with a conventional patterning method provides us with a novel route for fabricating patterned magnetic with a sub-lithographic length-scale. The process is promising for the fabrication of magnetic elements having high aspect ratios. However, it may be hard to control the length distributions of short magnetic pillars [2].

#### **f) Templated Dewetting of Magnetic Thin Films**

Dewetting of magnetic thin films on topographically modified substrates is another templated self-assembly process with an ultimate goal to fabricate well-ordered magnetic elements. As discussed in Part I continuous thin films deposited on flat surfaces break up into islands on annealing [55, 56]. The fabricated particles do not exhibit any long-range order. However, the effect of the substrate is significant and forces the ordering of the fabricated particles [20, 21]. Like in every templated

self-assembly process, the desired material can be self-organized on a surface patterned with conventional lithography leading to long-range periodic structures with a smaller length scale than that of the initial pattern.

As already discussed, the fabricated nanoparticles are topographically confined and it is speculated that this might prevent agglomeration or coarsening during any subsequent high-temperature growth. Moreover, they exhibit uniform in-plane and out-of-plane orientation as a result of the modified topography. In case of magnetic elements, this means that we can take advantage of their magnetocrystalline anisotropy and magnetize them either in- or out-of-plane. Two necessary conditions are that their easy magnetic axis lies in-plane or out-of-plane correspondingly, and that the magnetocrystalline anisotropy will be high enough to avoid superparamagnetic behavior at large sizes.

A significant question which remains unanswered is whether templated dewetting technology can force the fabrication of magnetic elements with shape anisotropy. Nanoparticles with almost spherical shape have been fabricated by dewetting of metal thin films in templates created by interference lithography [20, 21]. The template was a periodic square array of holes created by two exposures at a  $90^\circ$  relative orientation. If we want to create templates with in-plane shape anisotropy, some modification of the interference lithography exposure is required [22]. The first option is to use a different dose (the product of the incident light's intensity by the exposure time) in the first and second exposure. Another possibility is to use exposures of two different periods. A final option is to use two off-orthogonal exposures of equal periods. However, it is not clear whether dewetting will result in periodic arrays of elements with in-plane shape anisotropy or more than one spherical particle will form in each topographical feature. The dewetted particles tend to have a

spherical shape in order to minimize their surface energy. Therefore, the ability of dewetting to fabricate magnetic particles with shape anisotropy (either in plane or out-of-plane) is still under question.

Another limitation of the templated dewetting process comes from the fact that the deposited polycrystalline thin must be continuous. However, this is an addressable limitation. As discussed in section 2.3.4, modifications of the deposition process can result in continuous thin films at a smaller thickness.

#### **4.4.4 The Uniform Texture of Dewetted Nanoparticles**

As it was thoroughly discussed in Chapter 2, dewetting of gold thin films on surfaces with di-periodic topography has produced well-ordered arrays of nanoparticles with uniform in-plane and out-of-plane orientation. The out-of-plane orientation of the fabricated nanoparticles is  $\{100\}$ , instead of a  $\{111\}$  texture as expected on a flat substrate according to the surface minimization condition for face-centered cubic (FCC) thin films [48]. The change of the texture is a direct consequence of the topographical features of the substrate and has been experimentally verified by XRD pole figure measurements [20, 21]. The goal of this section is to discuss whether the texture of the dewetted nanoparticles can be useful for the fabrication of patterned magnetic media.

As discussed in section 4.2.1, the easy magnetization axis of the magnetic nanoparticles must coincide with the direction of the writing field. Neglecting shape effects (we can assume spherical particles since there is no evidence that dewetting can produce nanoparticles with shape anisotropy), the easy axis of magnetization is determined by the crystalline structure of the medium. For FCC metals the easy axes are parallel to the  $\langle 111 \rangle$  directions. The  $\{100\}$  texture is undesirable for the

fabrication of a stable magnetic medium. We have to apply a magnetic field at an angle defined by the angle between the  $\langle 100 \rangle$  and  $\langle 111 \rangle$  directions, in order to take advantage of the magnetocrystalline anisotropy of the FCC particles. This is an unpractical solution. Templated dewetting of FCC films can be useful for the fabrication of magnetic media only if it can result in well-ordered arrays of nanoparticles with a  $\{111\}$  texture. It is a future challenge to dewet thin films on templates with different topographies with the ultimate goal to fabricate nanoparticles with the desired texture.

The  $\{111\}$  planes of an FCC metals are equivalent to the (0001) planes of an HCP metal. Therefore, it is speculated that dewetting of an HCP film (e.g. Co) in the templates fabricated by the experimental steps of Table 2-1 will not result in the desirable (0001) texture.

In conclusion, thin film dewetting can be useful for the fabrication of patterned magnetic media only after the satisfaction of a necessary condition: the resulting texture of the nanoparticles must be normal to the easy axis of magnetization. This will facilitate the easy application of an external magnetic field. Another alternative is to produce particles with shape anisotropy but this is also doubtful.

#### **4.4.5 The Superparamagnetic Limit of Dewetted Nanoparticles**

According to the viability limit of the patterned media, the fabricated nanoparticles should have a maximum periodicity of 50 nm (section 4.3.1). In order to avoid interactions between neighboring elements, their diameters should be on the order of half of the period of the array, i.e. 25 nm (section 4.3.3). This is the maximum size of the particles which should be achieved by the templated dewetting

technology. In order to fabricate nanoparticles with sizes in the above regime, it is expected that we would probably have to deal with a discontinuous thin film, which would dewet to form random arrays of particles. However, as already mentioned, we might decrease the minimum thickness of a continuous thin film by the modifying the parameters of the deposition process (section 2.3.4).

According to the previous paragraph, the maximum dimensions of patterned media are determined by the viability limit. Moreover, their minimum dimensions are determined by their superparamagnetic behavior. The rate of switching of their magnetization is given by an Arrhenius-Néel-type law [2, 49]:

$$\tau^{-1} = f_0 \exp(-\Delta E/kT) \quad (\text{Eq. 4.5})$$

The quantity in the exponential is the stability criterion which was mentioned in the paragraphs 4.1.1 and 4.1.2.  $\Delta E$  is the energy barrier for reversal and  $f_0$  is an attempt frequency typically taken as  $10^9 \text{s}^{-1}$ . According to manufacturers [3] and researchers [2, 50, 51], an acceptable magnetic medium should have a stability ratio in the order of 60. The value of this ratio can determine the minimum acceptable size of the magnetic elements in order to have a thermally stable patterned medium. If the magnetic elements have uniaxial magnetic anisotropy, then the energy barrier for magnetization reversal is equal to  $KV$ . However, if the magnetic elements have cubic anisotropy (as in the case of Ni or Fe), then  $\Delta E=KV/4$  for materials with  $\langle 100 \rangle$  easy magnetization axes (e.g. Fe), and  $\Delta E=KV/12$  for materials with  $\langle 111 \rangle$  easy magnetization axes (e.g. Ni) [49, 52].

Using the values of the anisotropy constants, we can calculate the minimum size of thermally stable magnetic nanoparticles fabricated by templated dewetting.

The following analysis will consider Fe, Ni and Co nanoparticles. The shape anisotropy effects will be ignored, since it is doubtful that we can obtain particles with anisotropic shapes using templated dewetting. In all cases we will consider room temperature operation ( $T=300\text{K}$ ) and the dewetted nanoparticles will be approximated as perfect spheres ( $V=4/3\times\pi(d/2)^3$ ). The value of the stability ratio will be considered equal to 60.

It is easily calculated that the minimum diameter of magnetic elements which will yield a stability ratio within the acceptable limits is: 10 nm for Co nanoparticles, 34 nm for Fe nanoparticles and 108 nm for Ni nanoparticles. We can see that only the dewetting of Co nanoparticles is of actual importance, since the value of the diameters for Fe and Ni nanoparticles are over the maximum limit determined by the viability of the medium. The magnetocrystalline anisotropy of Fe and Ni is so low that it cannot facilitate the fabrication of a patterned medium without the contribution of shape anisotropy. It should be once again stated, that shape anisotropy effects were ignored for the above calculations and the dewetted particles were approximated as perfect spheres.

#### **4.5 Conclusions**

The fabrication of patterned media by the templated dewetting of metal thin films could be possible. However, it involves some inherent difficulties and many critical questions remain unanswered.

First of all, the uniform texture of the FCC dewetted particles, as demonstrated for Au nanoparticles by Giermann and Thompson, is not perpendicular to the easy axis of magnetization of an FCC nanoparticle [20]. Even if we could fabricate FCC nanoparticles (i.e. from nickel) with the desirable {111} texture, they would be

useless for the fabrication of viable patterned media, since they would experience thermal fluctuations and magnetization reversal at very large sizes. The same limitation applies to patterned media based on the magnetocrystalline anisotropy of iron. Of more interest could be the templated dewetting of cobalt films, which would produce nanoparticles with uniaxial magnetic anisotropy. The large magnetocrystalline anisotropy of cobalt enables Co nanoparticles to be suitable for the fabrication of patterned media if they have diameters between 10 and 25 nm. The maximum periodicity is determined by the viability limit (section 4.3.1) and it is equal to 50 nm. The minimum periodicity is determined by the interactions between neighboring magnetic elements and should be larger than the average diameter of the elements by at least a factor of two. It has not been yet demonstrated whether templated dewetting of cobalt films can give us nanoparticles with the desirable (0001) texture. It remains a future challenge to fabricate nanoparticles with the desired texture by investigating dewetting of Co films in templates with different topographies.

Moreover, it is difficult to fabricate particles within the above range of sizes by the dewetting of a continuous thin film. The initial thin film is expected to be discontinuous and it may dewet into random arrays of nanoparticles, ignoring the topographic template. As discussed in Part I, there are many possible modifications of the deposition process, which could result in a significant decrease of the minimum film thickness. Increasing the deposition rate and the background pressure, as well as decreasing the temperature of the substrate can yield a continuous film at a smaller thickness (section 2.3.4). The effect of the deposition parameters in determining the grain size at coalescence and the minimum thin film thickness has been modeled by Thompson [57].



It should be also noted that the limit of interference lithography is expected to be in the order of 50 nm. This regime can be reached by using achromatic interference lithography. For the fabrication of features with smaller sizes, another patterning technology should be used (electron beam lithography, X-Ray lithography, self-organized templates).

Another question which remains unanswered is whether the process of templated dewetting can fabricate structures with shape anisotropy. In this case, the net magnetic anisotropy of the particles can be higher and the technology will be more promising, as far as the fabrication of competitive patterned media is concerned.

## References

1. DUX Computer Digest, website : <http://www.duxcw.com>
2. C.A. Ross, *Annu. Rev. Mater. Res.*, **31**, p. 203 (2001).
3. Hitachi Global Storage Technologies, website : <http://www.hitachigst.com>
4. N. Spaldin in “*Magnetic materials: Fundamentals and device applications*”, Cambridge University Press (2003).
5. R.C. O’ Handley in “*Modern magnetic materials: Principles and Applications*”, Wiley-Interscience Publications (2000).
6. M. Farhoud, H.I. Smith, M. Hwang and C.M. Ross, *J. Appl. Phys.*, **87**, p. 5120 (2000).
7. C.A. Ross, H.I. Smith, T. Savas, M. Schattenburg, M. Farhoud, M. Hwang, M. Walsh, M.C. Abraham and R.J. Ram, *J. Vac. Sci. Technol. B*, **17** (6), p. 3168 (1999).
8. C.A. Ross, Massachusetts Institute of Technology, DMSE, MEng Lecture (July 18<sup>th</sup> 2001).
9. R. Ferre, K. Ounadjela, J.M. George, L. Pirauz and S. Dubois, *Phys. Rev. B.*, **56**, p. 14066 (1997).
10. J.M. Garcia, A. Asenjo, J. Velazquez, D. Garcia, M. Vazquez, P. Aranda and E. Ruiz-Hitzky, *J. Appl. Phys.*, **85**, p. 5480 (1999).
11. W. Schwarzacher, O.I. Kasyutich, P.R. Evans, M.G. Darbyshire, G. Li, V. M. Fedosyuk, F. Rousseaux, E. Cambril and D. Decanini, *J. Magn.Magn. Mater.* **198**, p. 185 (1999).
12. S. Pignard, G. Goglio, A. Radulescu, L. Piraux, S. Dubois, A. Declémy and J. L. Duvail, *J. Appl. Phys.*, **87**, p. 824 (2000).

13. M. Thielen, S. Kirsch, H. Weinforth, A. Carl and E.F. Wassermann, *IEEE Trans. Magn.*, **34**, p. 1009 (1998).
14. R.P. Cowburn, *J. Phys. D*, **33**, p. R1 (2000).
15. S. Evoy, D.W. Carr, L. Sekaric, Y. Suzuki, J.M. Parpia and H.C. Craighead, *J. Appl. Phys.*, **87**, p. 404 (2000).
16. C.A. Ross, M. Farhoud, H.I. Smith, M. Hwang, M. Redjidal and F. Humphrey, *J. Appl. Phys.*, **89**, p. 1310 (2001).
17. F. Rousseaux, D. Decanini, F. Carcenac, E. Cambriil, M.F. Ravet, C. Chappert, N. Bardou, B. Bartenlian and P. Veillet, *J. Vac. Sci. Technol. B* **13**, p. 2787 (1995).
18. W. Wernsdorfer, K. Hasselbach, D. Mailly, B. Barbara, A. Benoit, L. Thomas and G. Suran, *J. Magn. Magn. Mater.*, **145**, p. 33 (1995).
19. C. Haginoya, K. Koike, Y. Hirayama, J. Yamamoto, M. Ishibashi, O. Kitakami and Y. Shimada, *Appl. Phys. Lett.*, **75**, p. 3159 (1999).
20. A.L. Giermann and C.V. Thompson, *Appl. Phys. Lett.*, **86**, p. 121903 (2005).
21. A.L. Giermann and C.V. Thompson, *Mat. Res. Soc. Symp. Proc.*, **818**, p. M3.3.1, (2004).
22. M.E. Walsh, Massachusetts Institute of Technology, Department of Electrical Engineering, Master of Science Thesis (2000).
23. M. Chou, P.R. Wei, P.B. Krauss and J. Fisher, *J. Vac. Sci. Technol. B*, **12**, p. 3695 (1994).
24. S. Y. Chou, *Proc. IEEE*, **85**, p. 652, (1997).
25. J.F. Smyth, S. Schultz, D.R. Fredkin, D.P. Kern, S.A. Rishton, H. Schmid, M. Cali and T.R. Koehler, *J. Appl. Phys.*, **69**, p. 5262 (1991).

26. R. O'Barr, R.M. Lederman, S. Schultz, W. Xu, A. Scherer and R.J. Tonicci, *J. Appl. Phys.*, **79**, p. 5303 (1996).
27. R. O'Barr, S.Y. Yamamoto, S. Schultz, W. Xu and A. Scherer, *J. Appl. Phys.*, **81**, p. 4730 (1997).
28. J. Wong, A. Scherer, M. Todorovic and S. Schultz, *J. Appl. Phys.*, **85**, p. 5489 (1999).
29. W. Wu, B. Cui, X. Sun, W. Zhang, L. Zhuang, L. Kong and S.Y. Chouet, *J. Vac. Sci. Technol. B*, **16**, p. 3825 (1998).
30. Molecular Imprints Inc., website : <http://www.molecularimprints.com>
31. T.A. Savas, M. Farhoud, H.I. Smith, M. Hwang, C.A. Ross, *J. Appl. Phys.*, **85**, p. 6160 (1999).
32. G. Zangari and D.N. Lambeth, *IEEE Trans. Magn.*, **33**, p. 3010 (1997).
33. R.M. Metzger, V.V. Konovalov, Ming Sun, Tao Xu, G. Zangari, Bin Xu, M. Benakli and W.D. Doyle, *IEEE Trans. Magn.*, **36**, p. 30 (2000).
34. M. Hwang, M.C. Abraham, T.A. Savas, H.I. Smith, R.J. Ram and C.A. Ross, *J. Appl. Phys.*, **87**, p. 5108 (2000).
35. R.M.H. New, R.F.W. Pease and R.L. White, *J. Magn. Magn. Mater.*, **155**, p. 140 (1996).
36. G.M. May and S.M. Sze in "*Fundamentals of Semiconductor Fabrication*" John Wiley & Sons Inc. (2004).
37. "*Introduction to Nanoscale Science and Technology*" Edited by M. Di Ventra, S. Evoy and J.R. Heflin Jr., Kluwer Academic Publishers (2004).
38. T. Kohda, Y. Otani, V. Novosad, K. Fukamichi and S. Yuasa, *IEEE Trans. Magn.*, **35**, p. 3472 (1999).

39. B. Cui, W. Wu, L. Kong, X. Sun and S.Y. Chou, *J. Appl. Phys.*, **85**, p. 5534 (1999).
40. G. Meier, M. Kleiber, D. Grundler, D. Heitmann and R. Wiesendanger, *Appl. Phys. Lett.*, **72**, p. 2168 (1998).
41. A. Fernandez, M.R. Gibbons, M.A. Wall, C.J. Cerjan, *J. Magn. Magn. Mater.*, **190**, p.71 (1998).
42. M.A.M. Haast, J.R. Schuurhuis, L. Abelmann, J.C. Lodder and Th.J. Popma, *IEEE Trans.Magn.*, **34**, p. 1006 (1998).
43. S. Xiao, X. Yang, E.W. Edwards, Y. La and P.F. Nealy, *Nanotechnology*, **16**, p. S324 (2005).
44. K. Naito, H. Hieda, M. Sakurai, Y. Kamata and K. Asakawa, *IEEE Trans. Magn.*, **38**, p. 1949 (2002).
45. J.Y. Cheng, C.A. Ross, E.L. Thomas, H.I. Smith and G.J. Vansco, *Adv. Mater.*, **15**, p. 1599 (2003).
46. R.A. Segalman, H. Ykoyama and E.J. Kramer, *Adv. Mater.*, **13**, p. 1152 (2001).
47. R. Krishnan, H.Q. Nguyen, C.V. Thompson, W.K. Choi and Y.L. Foo, *Nanotechnology*, **16**, p. 841 (2005).
48. C.V. Thompson, *Annu. Rev. Mat. Sci.*, **30**, p. 159 (2000).
49. M. Walker, P.I. Mayo, K. O'Grady, S.W. Charles and R.W. Chantrell, *J. Phys.: Condens. Matter*, **5**, p. 2779 (1993).
50. T.W. McDaniel, *J. Phys.: Condens. Matter*, **17**, p. R315 (2005).
51. S.H. Charap, Pu-Ling Lu and Y. He, *IEEE Trans. Magn.*, **33**, p. 978 (1997).
52. M.P. Pileni, *Adv. Funct. Mat.*, **11**, p. 323 (2001).
53. Z.J. Sun and H.K. Kim, *Appl. Phys. Lett.*, **81**, p. 3458 (2002).

54. R. Krishnan, K. Nielsch, C.A. Ross, H.I. Smith and C.V. Thompson,  
*Electrochemical Society Meeting* (Orlando Oct. 2003).
55. E. Jiran and C.V. Thompson, *J. Electron. Mater.*, **19**, p. 1153 (1990).
56. E. Jiran and C.V. Thompson, *Thin Solid Films*, **208**, p. 23 (1992).
57. C.V. Thompson, *J. Mater. Res.*, **14**, p. 3164 (1999).

## 5. Catalytic Growth of Semiconducting Nanowires

### 5.1 Introduction

Nanowires (NWs) are one-dimensional structures with diameters of 3 – 100 nm and up to several  $\mu\text{m}$  in length [1]. They can serve as a basis for creating new devices based on quantum mechanics [2], as well as for probing the physics of one-dimensional transport. A great variety of different materials has been utilized for the fabrication of semiconducting NWs. Nanowires have been fabricated from elemental semiconductors (Si, Ge) [3, 4], III – V semiconductors (GaAs, GaP, InP, InAs) [5, 6], II-VI Semiconductors (ZnS, ZnSe, CdS, CdSe) [7] and oxides (ZnO, MgO, SiO<sub>2</sub>) [8]. Nanowires with variable doping (n-Si/p-Si, n-InP/p-InP) [9] and variable composition (InAs/InP, GaAs/GaP, Si/SiGe) [10] have been demonstrated.

A great variety of applications of semiconducting nanowires has been demonstrated including field-effect transistors [11], rectifiers [12], photodetectors [13], bio/chemical sensors [14], LEDs [12, 15], nanowire lasers [16], logic devices [17, 18] and as substrates for photocatalysis and photovoltaics [19].

The purpose of this section is to discuss whether the templated dewetting process could be a useful technology for the fabrication of well-aligned semiconducting nanowire arrays. Random nanowire arrays are undesirable for the fabrication of electronic and optoelectronic devices, since we would have no control over the results of the fabrication process and we would be unable to address the individual components (transistors, LEDs, logic devices etc.). As already discussed, templated dewetting can produce regular arrays of metal nanoparticles with uniform crystallographic orientation. The question is if we can take advantage of the above characteristics of the dewetted particles and use them as catalysts for the growth of

aligned semiconducting nanowire arrays. The catalytic behavior of metal nanoparticles is described by the well-known VLS mechanism, which is described in the following paragraph.

## **5.2 VLS Growth Mechanism**

### **5.2.1 Description**

The most widely accepted mechanism for the growth of semiconducting nanowires was proposed by R.S. Wagner and W.C. Ellis in 1964 and it is known as the Vapor – Liquid – Solid (VLS) mechanism [20].

According to the VLS mechanism, a metallic nanoparticle (e.g. gold) is placed on a substrate (e.g. {111} silicon wafer) and is heated above the eutectic temperature of Au-Si system. The result is the formation of a Au-Si droplet. A mixture of gases containing a source gas for growth of the semiconductor, (e.g. SiCl<sub>4</sub> accompanied by H<sub>2</sub>) is introduced into the furnace. The liquid surface is a preferred site of deposition for the incoming silicon vapor. When the liquid alloy becomes supersaturated with Si, a silicon nanowire can grow by precipitation at the solid-liquid interface. The result is long Si nanowires with the metal catalyst at their tip, providing evidence for growth from the tip according to the VLS mechanism. The summary of the described process is illustrated in Figure 5-1. A similar route is followed for the growth of semiconducting nanowires of any material.



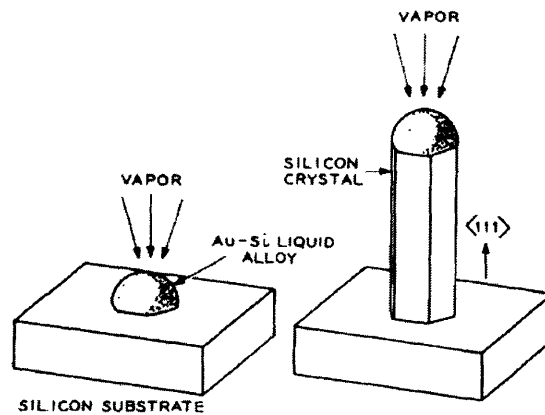


Figure 5-1: Illustration of the VLS growth mechanism. The source gas is introduced into the furnace and forms a liquid droplet with the metal catalyst. Supersaturation results in the nucleation of a vertically aligned semiconducting nanowire [20].

Depending on the generation of the vapor species, there can be many variations of the VLS mechanism. Both physical methods such laser ablation, arc discharge or thermal evaporation [10, 15, 21-23] and chemical methods such as chemical vapor deposition [19, 20, 22] have been used. Chemical vapor deposition (CVD) is the preferred technology if we have already deposited the metal catalysts on a substrate. On the other hand, laser ablation is used for the generation of the metal catalysts, as well as for the growth of the nanowires [21]. A lot of different nanoparticulate metals have been used as catalysts, including Au, Pt, Ag, Pd, Cu, Ni, Au-Pd and Fe [20, 21, 24].

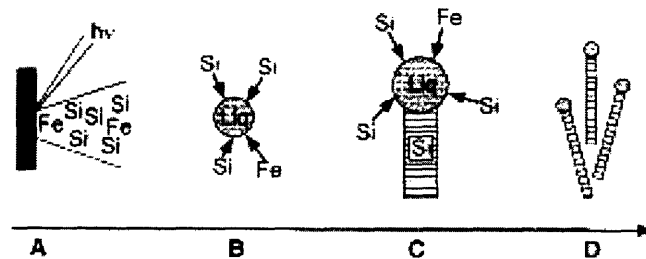


Figure 5-2: A laser ablation method for the fabrication of Si nanowires. (a) A target of Si and Fe is ablated by high-energy photons. (b) The vapor of Si and Fe condenses into Si-rich liquid catalysts. (c) Supersaturation results in the precipitation of Si. (d) The final nanowires [21].

There are two conditions which must be satisfied in order to obtain VLS growth. First of all, the catalysts and the desired NW material should form a eutectic. Secondly, the growth temperature should be higher than the eutectic point but lower than the melting point of the NW material. The original model of the VLS mechanism included dissolution and diffusion into the liquid phase and precipitation at the liquid-solid interface [20]. Another approach takes into account diffusion along the liquid-solid interface and subsequent precipitation [25].

We are specifically interested in the potential of templated dewetting for the growth of dense, well-ordered nanowire arrays, which will be oriented orthogonally to the {100} Si substrate. Therefore, we should discuss the factors which determine the growth direction of the NWs.

### **5.2.2 Control of the Growth Direction**

Each nanowire material has a preferred growth direction, which can be calculated considering the theory of kinetics. For example, silicon is a covalently bonded semiconductor. The enthalpic contribution to its total energy is much higher than the entropic contribution. Therefore, Si has a flat surface according to the energy minimization condition. As a material with a flat a surface, it grows following the ledge mechanism, which results in highly anisotropic growth rates [26]. According to Spaepen and Turnbull, the {111} surface has the lowest growth velocity for Si [27]. The result is the development of faceted crystals, which are bound by the slowest growing interfaces (which are {111}). Following the VLS mechanism, nanowires are grown by a typical nucleation & growth process. Therefore, the above results will apply and the grown Si nanowires will be characterized by a preferred growth direction (which is the  $\langle 111 \rangle$  direction).

According to the above considerations, Si nanowires can grow epitaxially and vertically only on (111) Si wafers. If we try to grow Si NWs on a (100) Si substrate, we will get three sets of oriented Si NW arrays along the three equivalent  $\langle 111 \rangle$  directions. Moreover, Si nanowires will grow randomly on an amorphous substrate (for example a Si substrate coated with SiO<sub>2</sub>) [19, 20, 22]. The substrate's orientation is one of the decisive factors for the orientation of the fabricated nanowires. Another factor that might affect the silicon growth direction is the topography of the substrate.

Considering the perfectly ordered nanoparticle arrays, which we acquired by the templated dewetting process, the VLS growth of NWs seems undesirable. We will be unable to take any advantage of the uniform crystallographic orientation of the nanoparticles, which might affect the alignment of the grown NWs, because it will be lost as soon as the metal catalysts turn into the liquid phase.

### **5.3 VSS Growth Mechanism**

#### **5.3.1 Description**

An alternative to the VLS mechanism was proposed recently by Persson et al. [28]. It is known as the Vapor – Solid – Solid mechanism (VSS) where the metal catalyst never turns into a liquid. The first experimental evidence for the VSS growth was demonstrated for the growth of GaAs nanowires using gold nanoparticles as catalysts. By a series of experiments, it is proven that both the wire and the seed particle show crystalline structure at all times, and a liquid phase is never observed.

However, even before the work of Persson et al. there was much evidence that a VSS nanowire growth could be possible. Earlier reports had demonstrated the growth of Ti-catalyzed Si nanowires and Au-catalyzed InAs nanowires, at

temperatures below the binary eutectic points [29, 30]. Moreover, the achievable abruptness of GaAs/InAs and InAs/InP hetero interfaces is in contradiction with the theory of the VLS mechanism and should be limited by the intermixing of the materials in the assumed molten alloy particle [1, 31].

### 5.3.2 Control of the Growth Direction

A series of experiments by Ohlsson et al. demonstrated that the growth direction of the fabricated nanowires depends on the phase of the catalyst [1]. They examined the growth of InAs nanowires and found out that at temperatures above the binary eutectic for Au-In the fabricated nanowires followed their preferred growth direction ( $\langle 111 \rangle$ ). However, when the growth temperature was lower than the eutectic binary point, the nanowires grew in random orientations.

The VSS growth is assumed to be the result of dissolution into the solid seed particle, followed by molecular diffusion to the interface between the seed particle and the nanowire and subsequent precipitation. It is therefore a nucleation & growth process, but the nucleation takes place in a solid matrix. Thus, we have to account for the misfit strain energy between the nanowire and the catalyst. It can be speculated that the strain energy minimization condition resulted in the dependence of the nanowire growth direction on the texture of the catalyst. That is why the nanowires lost their preferred growth direction and grew randomly. It should be also noted that Ohlsson et al. used aerosol deposited Au catalysts with non-uniform orientation. However, using the templated dewetting technology, we can have Au catalysts with uniform crystallographic orientation. The uniform orientation of the solid nanoparticles might influence the orientation of the grown nanowires and result in their alignment.

## 5.4 Conclusions

In terms of the nanowire growth, the key characteristic of the particles created by templated dewetting is their uniform crystallographic orientation. However, it is not clear from the existing literature, whether the orientation of the catalyst could influence the growth direction of the nanowires during the VSS growth. Nevertheless, it is clear that we should have a VSS growth if we want to take advantage of the uniform orientation of the dewetted nanoparticles. This requires continuous control over the temperature of the CVD chamber in order to avoid exceeding the binary eutectic temperature, which is determined by the nanowire material and the metal catalyst.

## References

1. B.J. Ohlsson, M.T. Björk, A.I. Persson, C. Thelander, L.R. Wallenberg, M.H. Magnusson, K. Deppert and L. Samuelson, *Physica E*, **13**, p. 1126 (2002).
2. Z. Zhong, F. Qian, D. Wang and C.M. Lieber, *Nano Lett.*, **3** (3), p. 343 (2003).
3. Y. Wu and P. Yang, *Chem. Mater.*, **12**, p. 605 (2000).
4. A.M. Morales and C.M. Lieber, *Science*, **279**, p. 208 (1998).
5. W. Han, S. Fan, W. Li and Y. Hu, *Science*, **277**, p. 1287 (1997).
6. T.J. Trentler, K.M. Hickman, S.C. Geol, A.M. Viano, P.C. Gibbons and W.E. Buhro, *Science*, **270**, p. 1791 (1995).
7. Y. Li, Y. Ding and Z. Wang, *Adv. Mater.*, **11**, p. 847 (1999).
8. M.H. Huang, Y. Wu, H. Feick, E. Webber and P. Yang, *Adv. Mater.*, **13**, p. 113 (2000).
9. M.S. Gudiksen, L.J. Lauhon, J. Wang, D.C. Smith and C.M. Lieber, *Nature*, **415**, p. 617 (2002).
10. X.F. Duan and C.M. Lieber, *Adv. Mater.*, **12**, p. 298 (2000).
11. Y. Cui and C. M. Lieber, *Science*, **291**, p. 851 (2001).
12. X.F. Duan, Y. Huang, Y. Cui, J.F. Wang and C.M. Lieber, *Nature*, **409**, p. 66 (2001).
13. J.F. Wang, M.S. Gudiksen, X.F. Duan, Y. Cui and C. M. Lieber, *Science*, **293**, p. 1455 (2001).
14. Y. Cui, Q.Q. Wei, H.K. Park and C.M. Lieber, *Science*, **293**, p. 1289 (2001).
15. D.P. Yu, Q.L. Hang, Y. Hing, H.Z. Zhang, Z.G. Bai, J.J. Wang, Y.H. Zou, W. Qian, G.C. Xiong and S.Q. Feng, *App. Phys. Lett.*, **73** (21), p. 3076 (1998).

16. M.H. Huang, S. Mao, H. Feick, H. Yan, Y. Wu, H. Kind, E. Weber, R. Russo and P. Yang, *Science*, **292**, p. 1897 (2001).
17. Y. Huang, X. Duan, Y. Ci, L.J. Lauhon, K. Kim and C.M. Lieber, *Science*, **294**, p. 1313 (2001).
18. A. Bachtold, P. Hadley, T. Nakanishi and C. Dekker, *Science*, **294**, p. 1317 (2001).
19. Y. Wu, H. Yan and P. Yang, *Topics in Catalysis*, **19** (2), p. 197 (2002).
20. R.S. Wagner and W.C. Ellis, *Appl. Phys. Lett.*, **4** (5), p. 89 (1964).
21. A.M. Morales and C.M. Lieber, *Science*, **279**, p. 208 (1998).
22. J.L. Liu, S.J. Cai, G.L. Jin, S.G. Thomas and K.L. Wang, *J. Cryst. Growth*, **200**, p. 106 (1999).
23. T. Kawano, Y. Kato, M. Futagawa, H. Takao, K. Sawada, M. Ishida, *Sens. Act. A*, **200**, p. 709 (2002).
24. Z.Q. Liu, W.Y. Zhou, L.F. Sun, D.S. Tang, X.P. Zou, Y.B. Li, C.Y. Wang, G. Wang and S.S. Xie, *Chem. Phys. Lett.*, **341**, p. 523 (2001).
25. H. Wang and G.S. Fischman, *J. Appl. Phys.*, **76** (3), p.1557 (1994).
26. C.V. Thompson, Massachusetts Institute of Technology, 3.205 Lecture Notes (2004).
27. F. Spaepen and D. Turnbull in “*Laser Annealing in Semiconductors*”, Edited By J.M. Poate and J.W. Mayer, Academic Press, NY, p. 30 (1982).
28. A.I. Persson, M.W. Larsson, S. Stenström, B.J. Ohlsson, L. Samuelson and R. Wallenberg, *Nature Mat.*, **3**, p. 677 (2004).
29. K. Hiruma, M. Yazawa, T. Katsuyama, K. Ogawa, K. Haraguchi, M. Koguchi and H. Kakibayashi, *J. Appl. Phys.*, **77**, p. 447 (1995).

30. T.I. Kamins, R. Stanley Williams, D.P. Basile, T. Hesjedal and J.S. Harris, *J. Appl. Phys.*, **89**, p. 1008 (2001).
31. M.T. Björk, B.J. Ohlsson, T. Sass, A.I. Persson, C. Thelander, M.H. Magnusson, K. Deppert, L.R. Wallenberg, and L. Samuelson, *Nano Lett.*, **2**, p. 87 (2002).



## 6. Catalytic Growth of Carbon Nanotubes

### 6.1 Introduction

The catalytic behavior of metal nanoparticles for the growth of one-dimensional structures is not limited to the fabrication of semiconducting nanowires. They can also act as catalysts for the growth of carbon nanotubes. In this section, the catalytic growth of carbon nanotubes will be discussed with special emphasis on the characteristics of the nanoparticles fabricated by templated dewetting. The goal is to determine whether the dewetted nanoparticles can be implemented for the fabrication of carbon nanotubes and the devices based on them.

A carbon nanotube (CNT) can be thought of as a hexagonal network of carbon atoms that has been rolled up to make a seamless cylinder (Fig. 6-1). While the cylinder is generally only a few nanometers across, it can be tens of  $\mu\text{m}$  long. Each of its ends is capped with half of a fullerene molecule. Single-wall nanotubes (SWNTs) can be thought of as the fundamental cylindrical structure, while multi-wall nanotubes (MWNTs) are essentially multiple SWNTs of different sizes that have formed in a coaxial configuration. Carbon nanotubes have extraordinary mechanical (Fig. 6-2) and electronic properties and hold great promise for future applications. The most important aspects of CNTs are their low density, high aspect ratio, one dimensionality, high mechanical strength and high electrical and thermal conductivity [1].

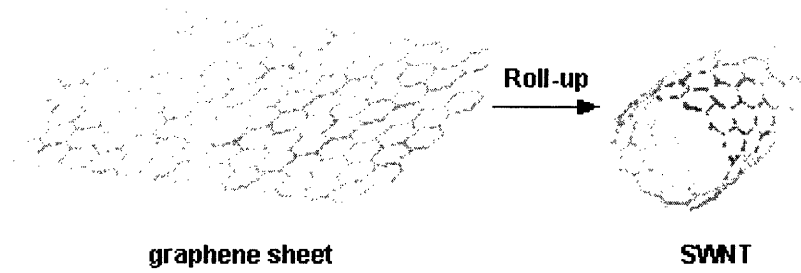


**Figure 6-1: A graphene sheet rolled into a Single-Wall Carbon Nanotube (SWNT) [2].**

Taking advantage of the impressive properties of CNTs, a huge variety of potential applications has been proposed. CNTs have been proposed as novel materials for the fabrication of scanning microscope probes [3], field-effect transistors [4], logic gates [5], quantum resistors [6], electromechanical sensors, bio/chemical sensors [1], hydrogen storage units [7] and field electron emitters in panel displays [8-13].

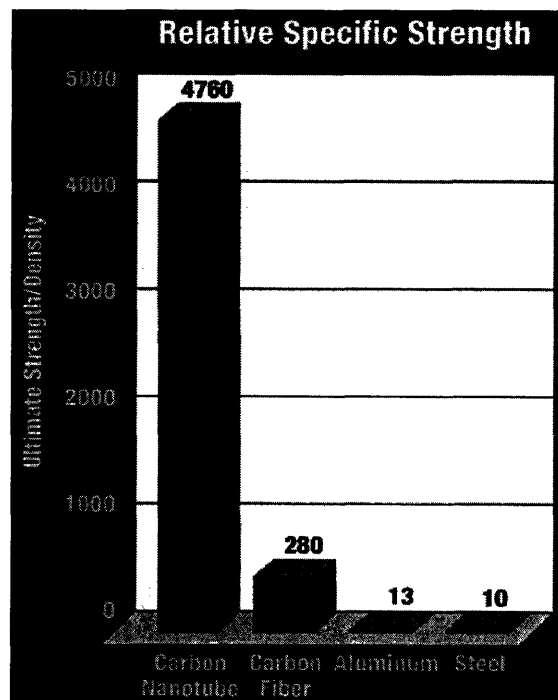


**Figure 6-2: An example of the remarkable mechanical properties of carbon nanotubes: A comparison of the specific strength of four different materials [14].**

## 6.2 Synthesis of Carbon Nanotubes

Carbon Nanotubes were first produced using arc discharge [15, 16] or laser ablation [17, 18]. Both of these methods were the first by which gram quantities of reasonably pure SWNTs were synthesized. Unfortunately, both also generate large quantities of byproducts (amorphous carbon, graphitic nanoparticles, fullerenes) and require high temperatures (3000° - 4000° C) [1].

Attempts to circumvent these inefficiencies have resulted in the development of a CVD process, in which gaseous carbon precursors come pyrolyzed to form single-wall and multi-wall nanotubes. The growth of CNTs is possible only if the CVD reaction is catalyzed by metal nanoparticles. There are two different methods for the generation of the metal catalysts. The precursors of nanoparticles can be organometallic gases, which decompose in the CVD reactor. Then the metallic part of the organometallic gas coarsens into nanoparticles, which can catalyze nanotube growth from the organic part. According to the second method, the metal catalysts are already deposited on a surface before the flow of the organic precursors into the reactor. Methane (CH<sub>4</sub>), acetylene (C<sub>2</sub>H<sub>2</sub>), ethylene (C<sub>2</sub>H<sub>4</sub>), ethanol, methanol, benzene and CO<sub>2</sub> have all been successfully pyrolyzed into SWNTs and MWNts by metal catalysts. The most widely used metal catalysts are Ni, Fe, Co and their binary alloys. NH<sub>3</sub> or H<sub>2</sub> are usually added to the reaction gas in order to etch the byproducts [19-27].

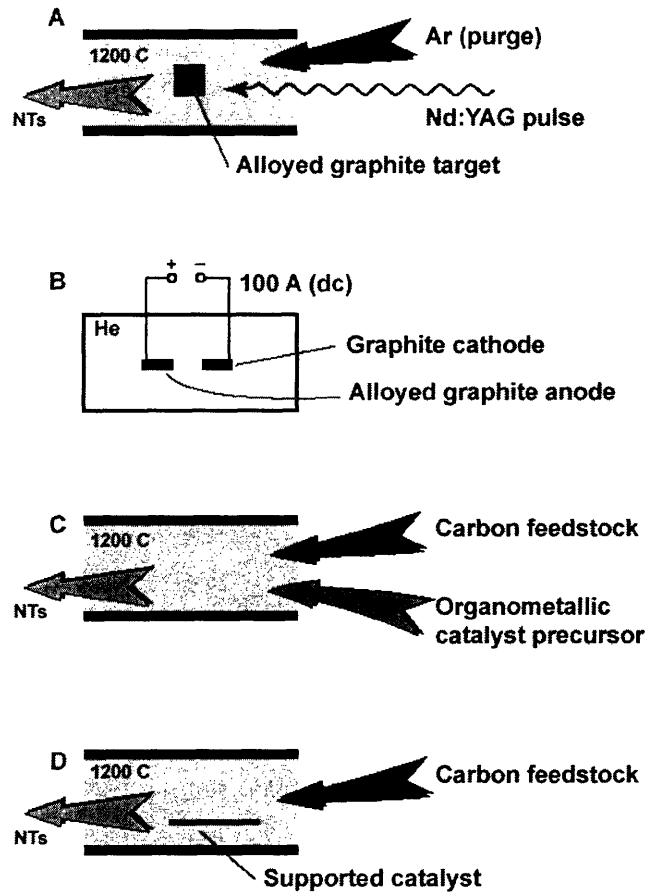


**Figure 6-3:** Four different techniques for the production of CNTs. (a) An alloyed graphite target is ablated by a Nd:YAG laser pulse. (b) Arc discharge results in the deposition of CNTs on the cathode. (c) Catalytic CVD process where the catalysts are generated by the decomposition of organometallic precursors. (d) Catalytic CVD process where the catalysts have been already deposited on a surface [1].

## 6.3 Growth Details

### 6.3.1 Growth Models

There are many models which have been proposed for the catalytic growth of carbon nanotubes. None of these models requires a liquid catalyst, as in the case of semiconducting nanowires. The catalyst never loses its crystallinity and carbon nanotube growth is considered a solid state process.

One of the most accepted mechanisms for the growth of CNTs is the ‘base growth’ mechanism. The catalyst serves as a nucleation site for a hemispherical cap and stabilizes the cap against closure. Carbon atoms are then added by direct absorption at the interface between the catalyst and the nanotube. Another possibility is the ‘tip growth’ mechanism. The tip-growth model involves a metal catalyst particle at a nanotube end being carried away as the nanotube lengthens. Thus, the carried-along particle is responsible for supplying carbon feedstock needed for the nanotube growth [28, 29]. The tip-growth mechanism resembles the VLS mechanism for the growth of semiconducting nanowires (with the difference that we now have a solid catalyst).

### **6.3.2 Growth Conditions – The Role of Dewetting**

The role of the metal catalyst and the growth temperature, have been experimentally correlated to the final products [1]. Specifically, nanoparticulate catalysts (0.8-1.2 nm in diameter) seem to be necessary for SWNT growth, while MWNTs can be formed in the presence of larger particles. However, if the particles are very large, carbon fibers are formed instead of MWNTs. Carbon fibers are graphite nanofibers which consist of very small graphite platelets, stacked in a perfectly arranged conformation (Figure 6-4). The particle size at which the transition from CNTs to carbon fibers is observed has not been quantitatively determined. However, for catalysts with diameters as large as 100 nm, carbon fibers are expected to be formed. High temperature favors the formation of SWNTs over MWNTs but it also causes the rapid coarsening of catalyst particles, thereby impeding SWNT production as the particles grow.

Templated dewetting can achieve the spatial confinement of the produced metal catalysts. Therefore, coarsening and agglomeration might be prevented. However, it has been already mentioned that the achievable particle size is limited by the thickness of the initial thin film. We need to have a continuous thin film in order to achieve a well-ordered distribution of the fabricated nanoparticles. The limitation of the minimum thin film thickness could be successfully addressed by modifying the deposition parameters, as described in section 2.3.4. The present technology of templated dewetting resulted in highly ordered arrays of particles with average diameter  $120.7 \text{ nm} \pm 1.14 \text{ nm}$  [30]. Particles within the above range of diameters are expected to catalyze the growth of carbon fibers, instead of CNTs. It is a technological and scientific challenge to scale-down the process of templated dewetting and fabricate particles which can catalyze the growth of multi-wall or even single-wall nanotubes.

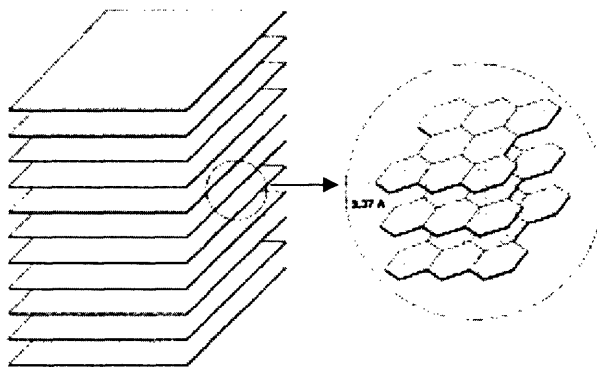


**Figure 6-4: Illustration of a carbon nanofiber [31].**

Templated dewetting results in the formation of ordered nanoparticle arrays with uniform crystallographic orientation. The crystallographic orientation of the catalyst (in combination with its shape) is expected to affect the chirality of the fabricated nanotubes. The chirality is the way a CNT is wrapped into a seamless cylinder and it is important, since it determines whether the tube will be metallic or

semiconducting. Experiments are under way to verify the correlation of the chirality to the orientation of the catalysts.

#### **6.4 Control of the Growth Direction**

Extensive studies have been made to determine the factors which influence the size and the alignment of the fabricated CNTs during CVD growth. The results have shown that the diameter of the carbon nanotubes is mainly determined by the diameter of the metal catalyst. However, there are many different factors which control the alignment of the tubes. These factors depend on the specific CVD technique used (thermo-CVD, plasma-enhanced CVD, hot filament CVD). In the case of PECVD, the alignment of the tubes is highly dependent on the magnitude of the applied voltage [27]. In the case of thermo-CVD or hot filament CVD, the alignment of the produced tubes is achieved by using arrays of catalysts which are very closely spaced to each other [28].

#### **6.5 Conclusions**

At the present stage of templated dewetting technology, the dewetted particles are so big that it is doubtful whether they can catalyze the growth of CNTs. Carbon nanofibers are expected to form instead. To achieve the catalytic growth of MWNTs, the described technology should be scaled down by decreasing the dimensions of the template and the initial thickness of the deposited film. For the production of SWNTs, we would need catalysts with diameters between 0.8 and 1.2 nm. Particles in above range of sizes have not been yet fabricated. However, by further experiments and continuous modification of the deposition parameters (section 2.3.4), the deposition of

a continuous thin film, which could dewet to form particles in the above size regime, may be possible.

As in the case of semiconducting nanowires, we aim at the fabrication of well-aligned regular arrays of CNTs. Random arrays of CNTs would be useless for the fabrication of devices, since it would be impossible to address the individual components. However, there is no experimental evidence that the alignment of CNTs depends on the crystallographic orientation of the catalysts. It is expected to be determined by the applied electrical fields or the magnitude of interparticle spacing. In the second case, we would acquire a bundle of CNTs touching each other.

The uniform crystallographic orientation of the dewetted nanoparticles might be important in determining the chirality of the fabricated tubes, and therefore their electronic properties. However, the above speculation has not been experimentally verified.

Finally, it should be noted, that the topographical confinement of the dewetted nanoparticles might prevent the coarsening of the catalysts, maintaining a regular interparticle spacing.



## References

1. "Introduction to Nanoscale Science and Technology" Edited by M. Di Ventra, S. Evoy and J.R. Heflin Jr., Kluwer Academic Publishers (2004).
2. "Nanotechnology Now", website : <http://www.nanotech-now.com>
3. S.S. Wong, J.D. Harper, P.T. Lansbury and C.M. Lieber, *J. Am. Chem. Soc.*, **120**, p. 603 (1998).
4. S.J. Tans, R.M. Verschueren and C. Dekker, *Nature*, **393**, p. 49 (1998).
5. V. Derycke, R. Martel, J. Appenzeller and Ph. Avouris, *Nano Letters*, **1**, p. 453 (2001).
6. S. Frank, P. Pancharal, Z.L. Wang and W.A. de Heer, *Science*, **280**, p. 1744 (1998).
7. S.M. Lee and Y.H. Lee, *Appl. Phys. Lett.*, **76**, p. 2877 (2000).
8. W.A. de Heer, A. Chatelain and D. Ugarte, *Science*, **270**, p. 1179 (1995).
9. J.M. Bonard, J. P. Salvetat, T. Stockli, L. Forro, and A. Chatelain, *Appl. Phys. A*, **69**, p. 245 (1999).
10. J.M. Kim, W. B. Choi, N. S. Lee, and J. E. Jung, *Diamond Relat. Mater.*, **9**, p. 1184 (2000).
11. W. Zhu, C. Bower, O. Zhou, G. Kochanski and S. Jin, *Appl. Phys. Lett.*, **75**, p. 873 (1999).
12. P.G. Collins and A. Zettl, *Appl. Phys. Lett.*, **69**, p. 1969 (1996).
13. S. Fan, M.G. Chapline, N.R. Franklin, T.W. Tombler, A.M. Cassell and H. Dai, *Science*, **283**, p. 512 (1999).
14. Easton Bicycle Components, website : <http://www.eastonbike.com>
15. S. Ijima, *Nature*, **354**, p. 56 (1991).

16. T.W. Ebbesen and P.M. Ajayan, *Nature*, **358**, p. 220 (1992).
17. T. Guo, P. Nikolaev, A.G. Rinzler, D. Tomanek, D.T. Colbert and R.E. Smalley, *J. Phys. Chem.*, **99**, p. 10694 (1995).
18. T. Guo, P. Nikolaev, A. Thess, D.T. Colbert and R.E. Smalley, *Chem. Phys. Lett.*, **243**, p. 49 (1995).
19. M.J. Yacamàn, M.M. Yoshida, L. Rendon and J.G. Santiesteban, *Appl. Phys. Lett.*, **62**, p. 202 (1993).
20. V. Ivanov, J.B. Nagy, Ph. Lambin, A. Lucas, X.B. Zhang, X.F. Zhang, D. Bernaerts, G. Van Tendeloo, S. Amelinckx and J. Van Landuyt, *Chem. Phys. Lett.*, **223**, p. 329 (1994).
21. X.Y. Song, W. Cao, M.R. Ayers and A.J. Hunt, *J. Mater. Res.*, **10**, p. 251 (1994).
22. N.M. Rodriguez, M.S. Kim and R.T.K. Baker, *J. Phys. Chem.*, **98**, p. 13108 (1994).
23. V. Ivanov, A. Fonseca, J.B. Nagy, A. Lucas, P. Lambin, D. Bernaerts and X.B. Zhang, *Carbon*, **33**, p. 1727 (1995).
24. A. Fonseca, K. Hernadi, J.B. Nagy, D. Bernaerts and A.A. Lucas, *J. Mol. Cat.*, **107**, p. 159 (1995).
25. H. Alvergnat, S. Bonnamy, A. Hamwi and F. Beguin, *Carbon 96, European Carbon Conference* (Newcastle, UK: July 7-12, 1996).
26. K. Ryu, M. Kang, Y. Kim and H. Jeon, *Jpn. J. Appl. Phys.*, **42**, p. 3578 (2003).
27. M. Chhowalla, K.B.K. Teo, C. Ducati, N.L. Rupesinghe, G.A.J. Amaratunga, A.C. Ferrari, D. Roy, J. Robertson and W.I. Milne, *Journal of Applied Physics*, **90**, p. 5308 (2001).
28. A. Huczko, *Appl. Phys. A*, **74**, p. 617 (2002).

29. J. Kong, H.T. Soh, A.M. Cassell, C.F. Quate and H. Dai, *Nature*, **395**, p. 878 (1998).
30. A.L. Giemann and C.V. Thompson, *Mat. Res. Soc. Symp. Proc.*, **818**, p. M3.3.1 (2004).
31. A. Chambers, C. Park, R. Terry, K. Baker, and N. M. Rodriguez, *J. Phys. Chem. B*, **102**, p. 4253 (1998).

***PART III: IP ANALYSIS AND BUSINESS MODEL***

## 7. Intellectual Property

### 7.1 Introduction

Before considering the commercialization of the templated dewetting process, we should analyze the intellectual property (IP) associated with it. According to the United States Patent and Trademark Office (USPTO), a patent is the grant of a property right to its inventor and is generally valid for 20 years after its filing date. During this time no other individual is permitted to “*make, use, offer for sale or sell the invention in the United States or import the invention into the United States*” [1]. Therefore, the MMNS Group could proceed with the commercialization of the templated dewetting technology only if no existing patent “blocks” the whole process or a specific experimental step. Otherwise, licensing or cross-licensing the rights of the blocking technology is a necessary condition before proceeding to commercialization.

The goal of this chapter is to identify any patents which pose IP obstacles that could prevent the unlicensed commercialization of the templated dewetting process. The database of the United States Patent Office served as the primary source for the survey [1]. This paper approaches the IP analysis by discussing the patents which are associated with different parts of the described technology. For the following analysis, the templated dewetting process was divided into three basic experimental steps: fabrication of topographic templates, deposition of the film and dewetting of the thin film into individual nanoparticles.

## **7.2 Patents Related to the Fabrication of Topographic Templates**

According to the experimental process which was discussed in Part I, interference lithography was used to fabricate the templates for subsequent thin film dewetting. However, other lithographic techniques such as electron beam lithography, X-Ray lithography and nanoimprint lithography could be used for the generation of the nanoscale patterns. The goal of this section is to evaluate if any valid patents on the potential patterning technologies exist that may require licensing for commercialization.

### **a) Electron Beam Lithography**

Electron beam lithography was developed in the 1970's. Its earliest form utilized a scanning electron microscope (SEM) for writing, while shaped electron beam lithography was invented some years later in order to improve the throughput of the process. The relevant patents were assigned to IBM and they have already expired [2, 3]. Electron beam lithography could be therefore used as the patterning method for the fabrication of the topographic templates without the need of licensing prior to potential commercialization.

### **b) X-Ray Lithography**

As described in section 4.4.2, X-Ray lithography is another candidate for the fabrication of nanoscale templates. It was also patented in the 1970's. In one of the earliest patents, Prof. Henry I. Smith claimed a '*Soft X-Ray lithographic apparatus and process*'. This patent was assigned to the Massachusetts Institute of Technology in 1973 [4]. In 1977 P.M. Eisenberg of the Bell Laboratories published a patent entitled '*X-ray photolithography*' [5]. These patents laid the principles of X-Ray

lithography. However, they are no longer valid. Thus, there is no associated blocking IP if the templates for the dewetting process are fabricated using X-Ray patterning.

#### **c) Nanoimprint Lithography**

Nanoimprint lithography is a novel patterning technique. It was first patented by S.Y. Chou in 1998 [6]. The claims of this patent contain all the details of the patterning technology and will remain valid until 2015. Therefore, unlicensed commercialization of the templated dewetting process is prohibited if nanoimprint lithography is used for the fabrication of the templates.

#### **d) Interference Lithography**

Interference lithography is the only patterning technology which has been used in the lab for the generation of the dewetting templates. It has been known since the late 60's due to the invention of the laser. Interference lithography has been also referred to as interferometric or holographic lithography. One of the first highly referenced patents was assigned to Texas Instruments in 1971 and was entitled '*Large Array Synthesizing*' [7].

Interference lithography has been heavily patented. This is mainly because of the many possible variations of the technique. Other highly referenced patents have been published by Prof. S.R.J. Brueck of the University of New Mexico [8] and Prof. H.I. Smith of M.I.T. [9, 10]. However, the patent which laid the principles of the process [7] has already expired and therefore there is no blocking IP associated with the fabrication of the dewetting templates by interference patterning.

### **7.3 Patents Related to the Deposition of Thin Films**

Electron beam evaporation has been experimentally used for thin film deposition on topographically modified substrates. Sputter deposition has been also proposed and relevant experiments are under way. As already mentioned, sputtered films are speculated to be continuous at smaller thickness in comparison to evaporated films. However, this speculation has to be experimentally verified for the case of the templated dewetting process.

Both of the above mentioned deposition techniques are well-known for many years. Their implementation is not expected to pose any IP difficulties on the potential commercialization of the templated dewetting process. The goal of this section is to verify the last speculation by lining up the results obtained from the USPTO database [1].

#### **a) Electron Beam Evaporation**

Electron beam evaporation for the deposition of metal thin films was first patented in 1972. The basic principles of the technology were described in a patent which was assigned to Bosch GmbH and entitled '*Metallic vapor deposition arrangement*' [11]. This patent is no longer valid and therefore it does not pose any IP obstacles to the commercialization of the templated dewetting process.

#### **b) Sputter Deposition**

The use of sputter deposition for the fabrication of the topographic templates does not prevent unlicensed commercialization of the templated dewetting process either. Sputter deposition was invented earlier than electron beam evaporation. As a vacuum deposition technology it has been in development since the late 1940's.



However, it didn't really pick up popularity until the semiconductor industry adopted it as a metal coating technique for conductive trace paths between transistors during the 1960's. According to the USPTO survey, the patent which lays the principles of the technology was filed in 1936. It was published as '*Coating by cathode disintegration*' and was assigned to Phillips [12].

#### **7.4 Patents Related to Rayleigh Instabilities and Thin-Film Dewetting**

The last step of the fabrication process is the dewetting of the deposited thin film and the formation of individual nanoparticles. A search of the USPTO database for patents related to Rayleigh instabilities and thin film dewetting was performed [1]. The terms 'dewetting', 'agglomeration', 'Rayleigh instabilities', 'capillary instabilities' were used for the above search. The goal was to find out if there are any unexpired patents directly related to the dewetting of thin films. A further search was conducted by using the names of the pioneers in this field (William W. Mullins, David J. Srolovitz, Carl V. Thompson). Both of the above searches yielded no results directly related to the dewetting process of thin films.

Most of the patents which are closely related to the Rayleigh instabilities take advantage of the theoretical analysis of Lord Rayleigh about the stability of a liquid jet, in order to fabricate uniformly sized liquid droplets [13-15]. In order to find patents related to the instability of thin solid films, a further search was conducted. The USPTO database was searched for patents related to the catalytic growth of carbon nanotubes. As mentioned in Chapter 6, CNTs have been synthesized by CVD reactions catalyzed by solid metal particles. The particles might have been generated by the deposition and dewetting of a thin film.

Most of the nanotube patents do not give details about the formation of the catalysts. However, US Patent # 6,764,874 [16], entitled '*Method for chemical vapor deposition of single walled carbon nanotubes*', claims a thin film dewetting process for the generation of the catalytic particles:

*"What is claimed is:*

*1. A method of fabricating nanotube structures comprising the steps of:*

*providing a substrate with a surface;*

*depositing a supporting layer on a surface of the substrate;*

*depositing an active catalyst film layer onto a surface of the supporting layer;*

*transforming the supporting layer into a plurality of supporting droplets and transforming the active catalyst film layer into a plurality of active catalyst nanoparticles which adhere to the supporting layer droplets using a reaction chamber having a growth temperature of less than 850.degree. C...." [16]*

The patent was filed by Motorola during 2003. However, it is not expected to pose any IP obstacles to the commercialization of the templated dewetting process, since it does not involve the use of any topographically modified template. Thin film dewetting is not a major claim of the patent. It is described as a part of the catalytic growth of SWNTs and no further reference is made.

In conclusion, there is a lack of Intellectual Property in the field of thin film dewetting. Little attention has been drawn into the exploitation of the dewetting phenomenon for the fabrication of useful devices, although the instability of thin films is well-known for about 20 years after the works of D.J. Srolovitz [17, 18] and C.V. Thompson [19, 20]. However, it was not until the work of A.L. Giemann and C.V. Thompson that the templated dewetting of metal thin films was introduced as a fabrication method for well-ordered nanoparticle arrays, which may prove useful for a

number of applications [21, 22]. According to the findings of the above USPTO search there is no patent related to the instability and dewetting of thin films, which inhibits the commercialization of the templated dewetting process

## **7.5 Conclusions**

The above patent analysis revealed that there are no significant IP restrictions in the field of templated dewetting. Dewetting of metal thin films is a novel area of research with very limited prior art. There are no IP restrictions associated with the deposition of thin films and their dewetting process. As far as the fabrication of the topographic templates is concerned, there can be restrictions if novel patterning methods, such as nanoimprint lithography, are used. In this case, the commercialization of the templated dewetting process could be possible only after licensing the rights of the patterning technique.

The MMNS Group could take advantage of the lack of intellectual property and patent all of the ideas they have developed. Publishing patents with broad claims would secure their place as a major player in the field and would provide protection against possible migration of the target market.

## References

1. United States Patent and Trademark Office, website : <http://www.uspto.gov>
2. US Patent # 3,644,700, International Business Machines Co. (1972).
3. US Patent # 4,099,062, International Business Machines Co. (1978).
4. US Patent # 3,743,842, Massachusetts Institute of Technology (1973).
5. US Patent # 4,028,547, Bell Telephone Laboratories, Inc. (1977).
6. US Patent # 5,772,905, Regents of the University of Minnesota (1998).
7. US Patent # 3,591,252, Texas Instruments Inc. (1971).
8. US Patent # 5,415,835, University of New Mexico (1995).
9. US Patent # 4,200,395, Massachusetts Institute of Technology (1980).
10. US Patent # 5,142,385, Massachusetts Institute of Technology (1992).
11. US Patent # 3,651,781, Robert Bosch GmbH (1972).
12. US Patent # 2,146,025, N.V. Phillips Gloeilampenfabrieken (1939).
13. US Patent # 5,266,098, Massachusetts Institute of Technology (1993).
14. US Patent # 6,116,516, Universidad de Sevilla (2000).
15. US Patent # 3,990,797, Xerox Co. (1976).
16. US Patent # 6,764,874, Motorola, Inc. (2004).
17. D.J. Srolovitz and S.A. Safran, *J. Appl. Phys.*, **60**, p. 247 (1986).
18. D.J. Srolovitz and S.A. Safran, *J. Appl. Phys.*, **60**, p. 255 (1986).
19. E. Jiran and C.V. Thompson, *J. Electron. Mater.*, **19**, p. 1153 (1990).
20. E. Jiran and C.V. Thompson, *Thin Solid Films*, **208**, p. 23 (1992).
21. A.L. Giermann and C.V. Thompson, *Mat. Res. Soc. Symp.*, **818**, p. M3.3.1 (2004).
22. A.L. Giermann and C.V. Thompson, *Appl. Phys. Lett.*, **86**, p. 121903 (2005).

## 8. Business Model

### 8.1 Empirical Evolution of Technology – Technological Barriers

The lack of blocking intellectual property opens the way for commercialization of the templated dewetting process. The goal of this chapter is to propose a business plan for each of the applications which were discussed in Part II. Plasmon waveguides will be excluded from the discussion because the templated dewetting process is not suitable for their fabrication. Before discussing the economic feasibility and proposing a business plan for each of the applications, the empirical evolution of the discussed technology will be presented in a graphical form (Fig. 8-1).

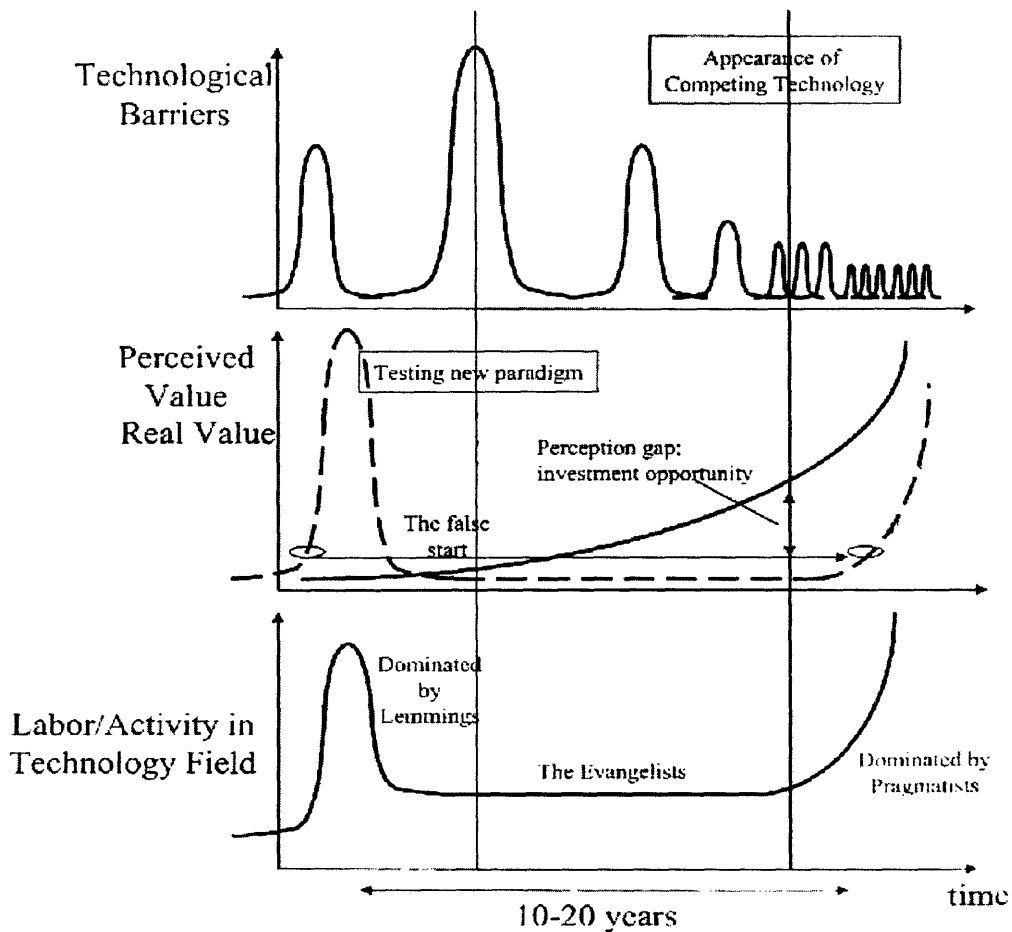


Figure 8-1: Empirical evolution of technology [1].

The first graph represents the technological barriers over time. The early big peaks represent the huge difficulties we need to overcome at the initial stage of research. Sometimes, there is a huge technological advance and it shows that the next barrier is even greater. As time passes, the difficulties are smaller but more frequent. In my opinion, the templated dewetting technology has overcome the initial big technological barriers. There is experimental evidence for the fabrication of well-ordered nanoparticle arrays. The testing of new paradigm, which determines the end of the first period of technological evolution, could be regarded as the substitution of the flat substrates with topographically modified substrates. However, there are still many challenges to face for the successful fabrication of patterned magnetic media and the catalytic growth of well-aligned arrays of wires and tubes. These challenges, such as scaling-down the process in order to fabricate particles which can catalyze the growth of tubes instead of fibers, maintaining a solid catalyst during nanowire growth and fabricating nanoparticles with the desired magnetocrystalline texture, were discussed in Part II.

The value of the investigated technology over the same period of time is represented in the second graph. The perceived value may include an initial peak characterized by over-investment in the described technology. The initial peak is known as the 'false start'. The perceived value drops off as soon as other technological barriers are recognized. The real value does not follow the 'false start' curve and soon becomes greater than the perceived value. This is because the second period of research is dominated by the 'Evangelists'. These are people who inform the general public about the ongoing laboratory research in order to draw their interest. The end of the second period is the best time for investment. The value of the perception gap will be the biggest, so the investors' revenues will be the highest.

The final plot contains information about the labor in the described field of technology. The first period is usually a period of hard work. This period is dominated by ‘Lemmings’, who blindly follow the crowd and do research on the technology. It includes the ‘false part’ and the testing of a new paradigm. The second period is dominated by the ‘Evangelists’ who inform the community about the ongoing research. The final period is dominated by the ‘Pragmatists’ who are trying to commercialize the results of the research.

As already noted, the dewetting technology for the fabrication of useful devices is at the beginning of the second period. A new paradigm (topographically modified substrate) has been already tested and proven successful. However, there are still many problems, which need to be overcome before the commercialization of any of the discussed applications could be possible.

## **8.2 Sustaining and Disruptive Technologies**

### **8.2.1 Definitions and Examples**

The first step in making a business plan is to identify whether the commercial products of the described technology will be a sustaining or disruptive force in the market. The current section will serve as an introduction to the above definitions and will follow the analysis of Prof. C.M. Christensen in his book “The Innovator’s Dilemma” [2]. In the next sections, the potential commercial products of the templated dewetting process will be categorized as ‘sustaining’ or ‘disruptive’ technologies.

According to Christensen, a sustaining technology is a new incremental technology which targets an established high-end market. For example, Pentium

microprocessors are a sustaining technology, since they replaced the similar 486 microprocessor technology, in the desktop PC market. Pentium microprocessors were designed to target the well established market of home computing. They provided higher clock speeds and they finally dominated over the market.

A disruptive technology targets emerging or low-end markets. It has a fundamentally different approach and is able to surpass the current technology without necessarily having a better performance. Christensen states that the major characteristic of a disruptive technology is that it emphasizes formerly overlooked attributes which are attractive to the consumers. For example, an InkJet printer could be regarded as a disruptive technology. InkJet printers were not designed to substitute LaserJet printers. They cannot offer a better performance in terms of speed or resolution. However, they took a large market share of the printers' sale, because they targeted a new market. The new market was the home computing market, which was asking for cheaper and smaller printers.

### **8.2.2 The 'Death-Zone' for Start-Up Companies**

The classification of the previous section is very important because it determines the business approach for an emerging technology. An innovator's business plans should be different for a sustaining than for a disruptive technology.

If a technology falls into the sustaining category, then it targets a well-defined high-end market with a lot of big competitors. Therefore, starting a new company based on a sustaining technology would not be a good option. According to Christensen, the fierce competition among the existing companies would be an insurmountable obstacle for the survival of a start-up [2]. The existing firms would do



everything to protect their profits and keep the consumers away from any new company.

On the other hand, a disruptive technology could enable the foundation of a start-up company. A disruptive technology targets low-end or emerging markets. Its competitors are fewer and smaller companies, or even non-consumption. There is no fierce competition which would make impossible the survival of a start-up company.

The above results are summarized by Christensen in the Figure 8-2. The upper-left section of the graph is characterized as the 'death-zone' for start-ups. It happens when the operation of a start-up company relies on a sustaining technological innovation. On the other hand, the effect of a disruptive technological innovation is depicted in the lower-right section of the chart. A successful start-up company should always target at an emerging market using existing or new technologies.

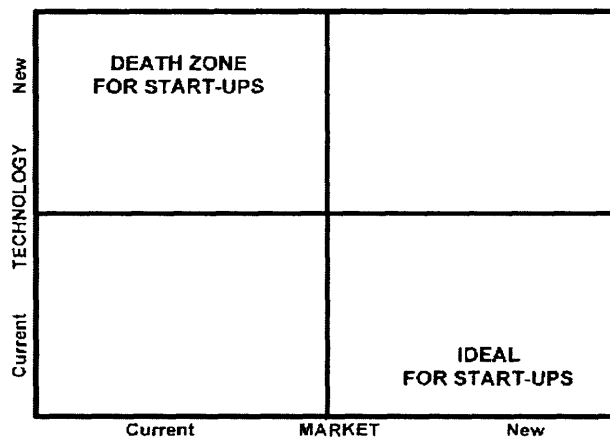


Figure 8-2: Chart indicating the ideal and death zones for start-up companies [2].

In conclusion, it would be unwise to found a start-up unless we are confident enough that our products will be a disruptive force in the market. Otherwise, we should find an alternative business plan for the generation of revenue. Licensing the developed technology to interested companies could be a wise solution. This could be

only possible by protecting the developing technology through the publication of patents. The manufacturing companies will be a sponsor for the academic research and will benefit from future profits. Large manufacturers interested in nanotechnology would be willing to invest in the templated dewetting technology even at an early stage. They can take this risk, since they do not need early revenues. Therefore, it would be very important for the MMNS of MIT to protect the templated dewetting technology by developing intellectual property.

In the following sections, we will discuss the business potential of each of the described applications of the templated dewetting process. We will identify the products which could be regarded as a disruptive force in the market, and we will propose a business plan for each of the potential applications.

### **8.3 Business Model Proposal**

#### **8.3.1 Commercialization of Patterned Magnetic Media – Sustaining or Disruptive Technology?**

##### **a) Patterned Media as a Sustaining Technology**

Before discussing the business potential of patterned media, we should stress once more the difficulties which were identified for the application of the templated dewetting technology in their fabrication. Overcoming these technological barriers must be our first priority. As already discussed, some of these barriers may be too high to overcome. The most important problem is the lack of experimental evidence that we can fabricate cobalt nanoparticles (or any other material with uniaxial magnetocrystalline anisotropy) with the desired crystallographic texture. The desired

crystallographic texture would be perpendicular to the easy magnetization axis of the magnetic particle. Another question is whether particles with shape anisotropy could be fabricated by the templated dewetting technology. The spherical shape of the nanoparticles is a direct result of the surface energy minimization condition. Therefore, the capability of dewetting to create anisotropic shapes is very doubtful. There are also further limitations associated with the limits of the patterning technology and the minimum initial thickness of the dewetted magnetic film.

Assuming that the above technological barriers could be overcome, we can proceed to discuss the marketability of patterned magnetic media. The main application of patterned magnetic media would be for hard disk drives (HDDs). Their ability to overcome the superparamagnetic limit of conventional longitudinal media could enable much higher areal densities. Patterned media is therefore targeting to the well-established HDD market with the ambition to replace the current magnetic media. An overview of the market size will clarify the intensity of the competition.

## **b) Market Analysis**

During 2004, the approximate revenues of the HDD market were \$22 billion. More than 250 million HDD units were shipped worldwide [3]. According to a recent study conducted by the International Data Group (IDC # 33432) worldwide HDD unit shipments and revenue will increase at a compound annual growth rate of 15.5% and 10.1% respectively from 2004 to 2009 [4].

Huge companies are the major players. The 2004 market share of the four largest HDD manufacturers is represented in table 8-1 [3]. The competition is so fierce that many manufacturers merge together to form giant companies. The most characteristic example is Hitachi Globe Storage Technologies formed by Hitachi and

IBM's HDD manufacturing section. Another example is the merger between Maxtor and Quantum. In 1985, there were 60 HDD manufacturers in the world. After mergers, acquisitions and bankruptcies, there now remain only seven. Owing to fast-changing technology, low profit margins, capital intensive research and development and the high bargaining power of PC manufacturers, this could reduce even further.

Company	Market Share
Seagate	34%
Maxtor	23%
Western Digital	14%
Hitachi Globe Storage Technologies	12%

**Table 8-1: Market share of the four largest HDD manufacturers (2004 data) [3].**

There are many companies which fabricate the magnetic media and supply their products to the final HDD manufacturers. Seagate and Hitachi Globe Storage Technologies fall into both categories, while Maxtor and Western Digital are fabricating only final HDDs. There is a fierce competition in the magnetic media market. The revenues of the market were as high as \$7.1 billion during 2004, while this value is expected to rise to \$9.3 billion in 2010 [5]. It should be noted that the vast majority of the current commercial magnetic media rely on conventional longitudinal thin film recording. At the end of 2004, Toshiba claimed the commercialization of the world's first HDDs based on perpendicular recording [6]. The patterned media technology is still at a laboratory scale.

In conclusion, the magnetic media market is a well-established high-end market. The fierce competition between the major players prevents the survival of any start-up company. Therefore, the preferred business plan for the commercialization of patterned media fabricated by templated dewetting would be to license the technology to interested manufacturing companies.

### **c) Patterned Media as a Disruptive Technology**

As it has been already discussed, patterned magnetic media is a sustaining technology, since it targets at the substitution of the conventional longitudinal media in the well-established HDD market. The unique characteristics of this market reveal certain conditions under which we can regard patterned media as a disruptive technology. Figure 8-3 illustrates the disruptive technological innovations in the HDD market for the past 30 years. Architectural changes were always the result of strong demand in an emerging market.

According to International Data Group experts, the HDD industry is again in transition [4]. The key driver of the market is the emerging market of consumer electronics (CE). Every home electronic device could contain a HDD as a means of data storage. The first consumer electronics products have already appeared in the market: portable digital music players which can store thousands of songs (e.g. Apple's Ipod), digital cameras with an ever-increasing storage capacity, novel cell phones which can contain hundreds of high-resolution pictures and videos, electronic game-machines which incorporate HDDs as a means of data storage. The above study predicts that worldwide consumer electronics HDD unit shipments will experience the fastest growth rate with a 37.4% compound annual growth rate over the next five years [4].

In conclusion, there is a strong emerging HDD market in consumer electronics. The market is not well-established yet but it is very promising. The survival and success of a start-up which targets the consumer electronics market could be possible, since the main competitor is non-consumption. Start-ups and existing companies are trying to make their products more and more attractive in order to draw the attention of new customers. Patterned media technology could enable higher

storage capacities and it could therefore be used for the fabrication of new portable HDD formats, which could satisfy the demand in the emerging consumer electronics market. A start-up based on this technology and targeting the consumer electronics market could be very promising.

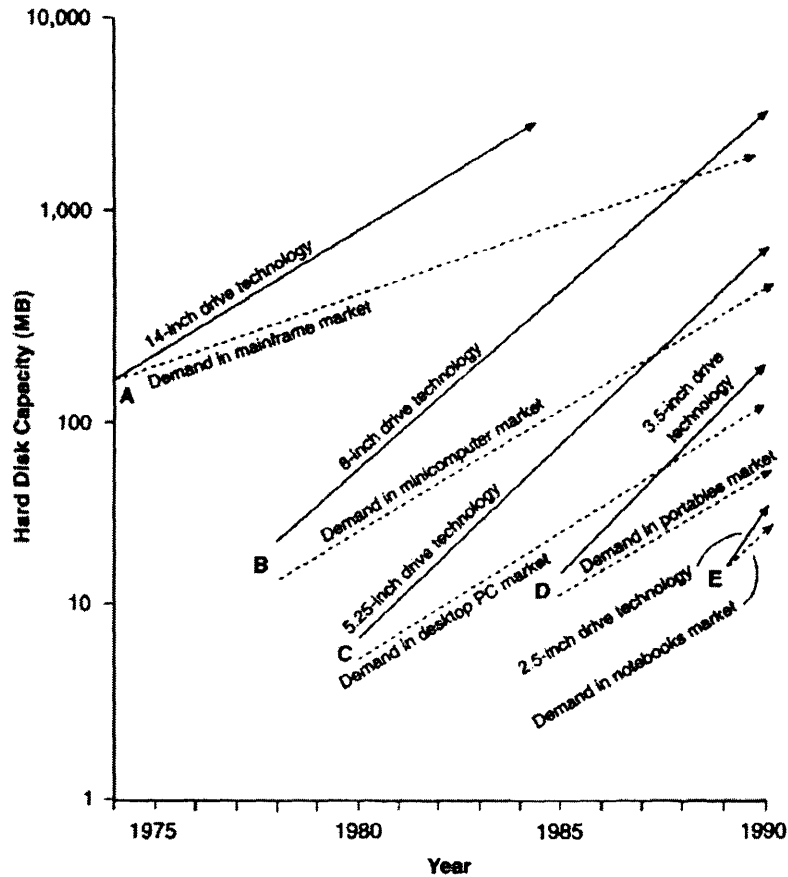


Figure 8-3: History of disruptive technological innovations in the HDD market [1].

#### d) Conclusions

Following the analysis presented in section 8.2.2, there are two possible business plans for the commercialization of patterned media. The first option is the development of intellectual property and the subsequent licensing of the templated dewetting technology to the interested manufacturing companies. These companies

will fund the university research and will benefit from the profits. The second option is the foundation of a start-up company which will target at the emerging consumer electronics market. The start-up would take advantage of the novel characteristics of the patterned media technology, which enable the fabrication of high-capacity HDD in novel portable formats. However, the commercialization of the templated dewetting technology for the fabrication of patterned magnetic media lies in the far future and could be possible only if the technological and scientific difficulties could be overcome.

### **8.3.2 Commercialization of the Applications Based on Well-Aligned Arrays of Nanowires and Nanotubes**

Nanoparticles fabricated by the templated dewetting process could catalyze the growth of aligned arrays of semiconducting nanowires (NWs) and carbon nanotubes (CNTs). As was discussed in Chapters 5 and 6, well-aligned nanowire arrays can serve as a basis for the fabrication of field-effect transistors, photodetectors, bio/chemical sensors, LEDs, logic gates, rectifiers and novel NW lasers. Moreover, nanotube arrays could find applications as quantum resistors, field effect transistors, scanning microscope probes, logic gates, field electron emitters, hydrogen storage units and electromechanical or bio/chemical sensors.

The above mentioned technologies are still at an embryonic stage. Current scientific research focuses on determining the factors which influence the growth parameters and the alignment of the fabricated nanostructures. The uniform crystallographic orientation of the dewetted nanoparticles might have a significant role in the above efforts. It is, however, clear that random arrays of one-dimensional nanostructures would be undesirable for the fabrication of commercial devices; since

we would have no control over the results of the fabrication process and we would be unable to address the individual components whether they are transistors, field emitters, LEDs, logic devices etc.

As far as the commercialization of the above devices is concerned, the analysis of the previous sections is still valid. It is very probable that these novel devices will enter the existing market as sustaining forces. Therefore, licensing of the developed technology would be the most successful business strategy. The MMNS Group of MIT would be advised to found a start-up company only if its products target at an emerging or low-end market.



## References

1. E.A. Fitzgerald, Massachusetts Institute of Technology, 3.207 Lecture Notes (2004).
2. C.M. Christensen in *"The Innovator's Dilemma"*, Harvard Business School Press (1997).
3. Responsive Database Services (Business & Industry Database), website : <http://rdsweb2.rdsinc.com>
4. International Data Group (IDC Market Research Database), website : <http://www.idgventures.com>
5. Business Communications Company Inc. (Research Reports), website : <http://www.bccresearch.com>
6. Toshiba Press Releases, website : <http://www.toshiba.com>

## 9. Thesis Conclusions

Templated dewetting of metal thin films is a promising route to nanofabrication. It can be combined with any patterning method and serve as a novel substitute for electrodeposition, evaporation and lift-off, or etching. It is still in an early stage of exploration and prior art is limited. However, the increasing scientific interest for nanoscale processes with self-assembly characteristics can be the driving force for more research in this field.

The major advantage of templated dewetting is the fabrication of well-ordered nanoparticle arrays with narrow size distribution and uniform crystallographic orientation. Moreover, the spatial confinement of the fabricated particles is speculated to prevent agglomeration or coarsening during high-temperature processing. On the other hand, the minimum feature dimension that can be achieved is determined by the resolution of the patterning technology and the minimum initial thickness of a continuous thin film.

Taking into account the above advantages and limitations, potential applications for the templated dewetting process were proposed and analyzed. The fabrication of competitive patterned magnetic media could be possible if the fabricated nanoparticles had uniaxial magnetic anisotropy and texture perpendicular to their easy axis of magnetization. Major technological challenges associated with the use of dewetting for patterned media fabrication is research on templates with different geometries and the attempt to acquire structures with shape anisotropy.

A vast range of applications depends on the use of the particles as catalysts for the fabrication of well-aligned arrays of semiconducting nanowires and carbon nanotubes. The catalytic growth of well-aligned arrays of semiconducting nanowires could be better controlled if we could ensure that the metal catalysts retain their

uniform crystallographic orientation by never turning into the liquid phase. The growth of carbon nanotubes depends on scaling down the process. Particles with the currently demonstrated diameters of 100 nm are expected to catalyze the growth of nanofibers. In order to obtain smaller nanoparticles which can catalyze the growth of multi-wall or even single-wall nanotubes, there should be a significant decrease in the minimum thickness of the deposited thin film. This limitation is addressable by modifying the parameters of the deposition process. Moreover, experiments are under way to prove that the orientation of the particles is crucial on determining the chirality of the fabricated tubes.

The process of dewetting is a potential candidate for the fabrication of plasmon waveguides. In this case, there is no need for a template. The fabrication of a waveguide depends on the dewetting of a one-dimensional structure according to the capillary instability theory. However, the spacing of the fabricated particles as determined by the instability theory is much larger than the optimum spacing for efficient light propagation. Therefore, the templated dewetting process is not considered to be a good route for the fabrication of plasmon waveguides.

The associated intellectual property is very limited and it is not expected to pose any serious obstacles to future commercialization of the templated dewetting process. All of the above applications are still at an embryonic stage and the remaining technological barriers are high. Throughout the evolution of technological developments, the accumulation of relevant IP is a necessary condition for the protection of the novel characteristics of the templated dewetting process.

All of the potential applications can enter the market as sustaining technological innovations. Therefore, the best option for commercialization is to license the rights of the process to the interested manufacturing companies. It would

be a good idea to proceed to the foundation of a start-up company only if the target application is expected to bring disruptive technological changes and aim at an emerging market. Such an example could be the novel market of Consumer Electronics which is expected to take advantage of the enhanced storage densities of patterned magnetic media.

Although the templated dewetting process is still at the very early stages of scientific research, it appears to be a promising technology. Overcoming the remaining technological barriers and optimizing the characteristics of the process could make it financially attractive to the major players in the field of nanofabrication.